Vortex Dynamics in Sharp Edged Domains

Author:
Mr. Graham BENHAM
Supervisor:
Prof. Robb MCDONALD

March 12, 2014

For my Father

Contents

Introduction

In this paper I will briefly summarise a few of the existing models for the behaviour of fluid flow and vortices near sharp-edged boundaries. I will focus my attention to the case of an inviscid fluid, for which there are two approaches I would like to consider. Johnson and McDonald (2004) used Hamiltonian methods to determine the dynamics near a gap in an infinitely long impermeable wall, however, this model does not account for a singularity in the velocity field at the tips of the boundaries of the order $(z - a)^{-\frac{1}{2}}$, as $z \to a$ (if a is the position of the tip). Therefore, it is necessary to impose the Kutta condition, that there must be finite velocity at the tip of the plate. By observation it is noted that for high Reynolds number flow past a sharp edge, a boundary layer is shed from the tip and takes the form of a vortex sheet whose trailing end rolls up into a spiral. You can witness this every time you turn a tea spoon in a mug of coffee or a kayak paddle in a river. Unfortunately the many attempts at mathematically modeling vortex sheets have revealed the unyielding nature of the complexities of the problem (Baker, 1980). However, using the Kutta condition and a conservation of momentum law, Brown and Michael (1954) derived an inviscid model for this viscous effect. An inviscid model is suitable considering a slender body because there are only viscous effects very close to the body and in the vortex shedding itself. They simulated the curled up sheet as a point vortex with unsteady circulation centered at the core of the spiral, and the vortex sheet itself as a branch cut in the complex plane which continuously feeds vorticity to the point vortex and over which there is a discontinuous jump in pressure. Cortelezzi (1995) used this method to derive an exact solution for the unsteady separated flow past a semi-infinite plate.

Chapter 1 will cover the derivation of the dynamics and equations that will be used throughout the paper. Chapter 2 will summarise the work of Johnson and McDonald (2004) on the gap problem, Chapter 3 will look at applications of the Brown-Michael model to flows past a semi-infinite plate. Chapters 4 and 5 will apply the same model to the case of gap in an infinite wall and a wedge of arbitrary angle.

Chapter 1

General Dynamics

The analysis of the problems in this paper will be in 2-dimensions and therefore it will be convenient to make use of the complex plane. In 2-dimensional inviscid fluid dynamics complex analysis is an invaluable tool. The domains to be investigated are non-trivial, that is to say, one cannot simply write down the complex velocity potentials using the method of images so that the impermeability boundary condition is satisfied on the wall, $v_n = 0$, where v_n is the velocity of the fluid in the normal direction to the wall. However, a conformal map from the physical plane to the upper half plane, otherwise known as the mathematical plane, allows us to find the complex velocity potential with considerable ease, for the image vortices are then simply the conjugate positions of the original vortices. Once the dynamics have been derived for the mathematical plane, one need only map the solution back to the original domain.

1.1 Hamiltonian Dynamics

The first approach to determining vortex dynamics is by constructing the vortex Hamiltonian. A useful tool for finding vortex trajectories is the Kirchoff-Routh function, Ψ (Saffman, 1995). For a system of N vortices at positions, z_j with circulations Γ_j, for $j = 1, \ldots N$, it is defined as:

$$\Psi = \frac{1}{2} \sum_{j \neq k}^{N} \Gamma_j \Gamma_k G\left(z_j, z_k\right) + \frac{1}{2} \sum_{j=1}^{N} \Gamma_j^2 G_H^{(j)}\left(z_j\right), \tag{1.1}$$

where $G_I\left(z, z_j\right) = G\left(z, z_j\right) + G_H^{(j)}\left(z, z_j\right)$ is the Green's function of the first kind, constituting of the freespace Green's function G and the harmonic function G_H. The first term of Ψ is the energy due to vortex-vortex interactions, whereas the second term is the energy of the vortices interacting with their images due to the boundary. In the specific case of $N = 1$, Ψ is also known as the Kirchoff-Routh Path function and at

constant values gives vortex trajectories. For $N \geq 1$, we can derive the equations of motion,

$$\Gamma_j \left(u_j - i v_j \right) = \frac{\partial \Psi}{\partial y_j} + i \frac{\partial \Psi}{\partial x_j}. \tag{1.2}$$

Therefore, if we define the phase-space coordinates,

$$q_i = \sqrt{|\Gamma_i|} \operatorname{sgn} \left(\Gamma_i \right) x_i, \tag{1.3}$$

$$p_i = \sqrt{|\Gamma_i|} \operatorname{sgn} \left(\Gamma_i \right) y_i, \tag{1.4}$$

we find that the Kirchoff-Routh function is in fact the Hamiltonian for the system:

$$\Psi = H(\mathbf{q}, \mathbf{p}) = H(\mathbf{z}) \quad ; \quad \mathbf{z} = \left(q_i, \ldots, q_N; p_i, \ldots, p_N \right), \tag{1.5}$$

since the real and imaginary parts of (1.2) yield the Hamiltonian equations of motion. If the conformal map $z = Z(\zeta)$ is such that $Z : \Omega \to \Omega'$, and H' is the Hamiltonian for the system in Ω', then we can find the Hamiltonian in Ω (Saffman, 1995) as,

$$H = H' + \sum_{j=1}^{N} \frac{\kappa_j^2}{4\pi} \log |Z'(\zeta_j)|. \tag{1.6}$$

The relationship between the Hamiltonian and the streamfunction ψ for a system of N vortices is,

$$H \left(\zeta_1, \ldots \zeta_N \right) = \sum_{j=1}^{N} \Gamma_j \psi \left(z_j \right). \tag{1.7}$$

1.2 Derivation of the Brown-Michael Equation

The fundamental element of this paper is the model which Brown and Michael used to simulate vortex shedding (1954). Originally they were trying to come up with a
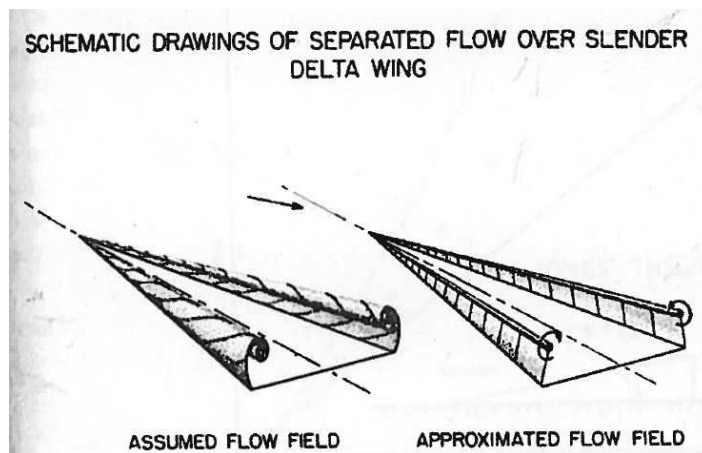

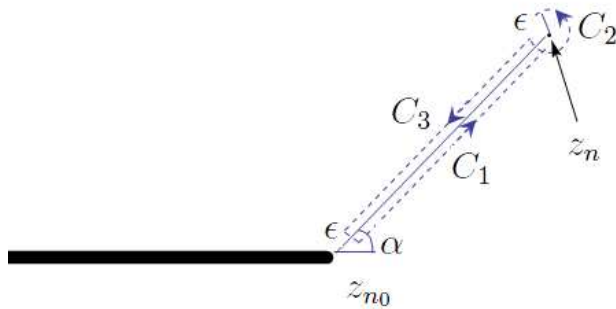
Figure 1.1: Taken from Brown. (1954)

Figure 1.2: Contour integral around the point vortex and its connecting cut, where α is the angle the line vortex makes with the horizontal and we take the limit as $\epsilon \to 0$.

simple model for analysing the effect of separated vortex sheets on the lift of a delta wing. In high Reynolds-number flow, conical vortex sheets can be observed to shed from the edge of a delta wing, with apex at the tip and base at the trailing edge. Across these sheets there is a large jump in the pressure and velocity of the fluid. The base of one of these vortex sheets is connected to the edge of the wing and its trailing edge curls up into a spiral. The sheet has variable shape and strength and continuously feeds vorticity to the spiral. In general it is thin and has relatively low circulation away from the spiral itself (see the assumed flow field in figure (1.1)).

By taking a 2-dimensional slice perpendicular to the axis of the delta wing, Brown and Michael (1954) developed an ingenious method for modeling this effect. In the 2-dimensional slice, in place of a curling vortex sheet we see a line vortex which begins at the wing edge and curls up into a spiral away from it. Given the thin and weak nature of the vortex sheet away form the spiral, they approximated this 2-dimensional system by a straight line vortex of negligible width connecting a point vortex to the tip of the plate, where the point vortex corresponds to the spiral and is centered at its core. The thin line vortex corresponds to the part of the vortex sheet which is not in the spiral (See figures (1.1) and (1.2)). It continuously feeds vorticity to the point vortex which is given variable strength and position. Along the thin line vortex there is a discontinuity in velocity and pressure, however, as a condition they imposed that the integral of pressure around the system must be zero. This translates to the condition that there must be zero net force on the point vortex and its connecting cut. Representing this model in the complex plane we would take a contour integral around the vortex system and apply Newton's second law. A second physical constraint is the so-called Kutta condition which states that the velocity at the trailing edge of a solid

body must be finite. We will use this condition throughout the paper to determine an equation for the unknown circulation of a shed vortex as a function of time.

We now outline the derivation of the equations of motion for a point vortex connected to the sharp edge of a solid body by a line vortex of negligible width along which there is a discontinuity in pressure (Llewellyn-Smith, 2009). If a fluid has velocity field $\underline{u} = (u, v)$, pressure p, density ρ and we take an arbitrary contour C with constant velocity $\underline{u_c} = (u_c, v_c)$, and normal vector $\underline{n}$, around the point vortex and its connecting branch, Newton's second law becomes

$$\frac{d\underline{M}}{dt} = \oint_C -p\underline{n}\,dl + \oint_C -\rho\underline{u}\left(\underline{u} - \underline{u_c}\right)\underline{n}\,dl, \tag{1.8}$$

because in 2-dimensions the change of momentum $\underline{M} = (M_1, M_2)$ is equal to the force on the contour from the fluid pressure plus the flux of momentum through the contour. We can convert this vector integral equation into a single scalar integral equation by making a change of variables to enter the complex plane. If $z = x + iy$, then $w = \frac{d\bar{z}}{dt} = u - iv$ gives the velocity field. If we consider a small change in x and y then we see that,

$$\underline{n}dl = -dy + idx, \tag{1.9}$$

and,

$$\begin{aligned}
\underline{u}.\underline{n}dl &= (-udy + vdx) \\
&= \tfrac{1}{2}\left(i\left(u - iv\right)\left(dx + idy\right) - i\left(u + iv\right)\left(dx - idy\right)\right) \\
&= \Re\left[iwdz\right]
\end{aligned} \tag{1.10}$$

Equation (1.8) gives us two integral equations, since it is a two dimensional vector, and we add them together in the manner $a + ib$ to give,

$$\frac{dM}{dt} = \oint_C -ip\,dz + \oint_C -\rho\left(u + iv\right)\Re\left[i\left(w - w_c\right)dz\right], \tag{1.11}$$

where $M = M_1 + iM_2$ and $w_c = u_c - iv_c$. If F represents the complex velocity potential for this flow, then Bernoulli's equation for the pressure is,

$$p = p_0(t) - \frac{1}{2}\rho\left(\frac{\partial F}{\partial t} + \frac{\partial \bar{F}}{\partial t} + w\bar{w}\right), \tag{1.12}$$

where p_0 is some analytic function of time and a bar represents the complex conjugate. Imposing the condition that the total force, or change of momentum, is zero and

substituting (1.12), we get,

$$\frac{i\rho}{2} \left(\oint_C (F_t + \bar{F}_t) \, dz + \oint_C w_c \bar{w} \, dz + \oint_C \bar{w} \, (\bar{w} - \bar{w}_c) \, d\bar{z} \right) = 0$$

$$\Rightarrow \quad \frac{i\rho}{2} \left(\underbrace{\oint_C (F_t + \bar{F}_t) \, dz}_{a} - \underbrace{\overline{\left(\oint_C \bar{w}_c w \, d\bar{z} \right)}}_{b} - \underbrace{\overline{\left(\oint_C w \, (w - w_c) \, dz \right)}}_{c} \right) = 0. \tag{1.13}$$

Now, if we let

$$w(z) = \frac{\Gamma_n}{2\pi i (z - z_n)} + \tilde{w}(z), \tag{1.14}$$

$$F(z) = \frac{\Gamma_n}{2\pi i} \log(z - z_n) + \tilde{F}(z), \tag{1.15}$$

where z_n is the position of the point vortex with circulation Γ_n and both $\tilde{w}$ and $\tilde{F}$ are analytic in C. It should be noted that the $\log(z - z_n)$ term in the complex velocity potential is singular at $z = z_n$ and therefore we make a branch cut along the connecting line and continue it along the sharp edge to $-\infty$. First, we see that,

$$a = \frac{i\rho}{2} \oint_C \left(\frac{\dot{\Gamma}_n}{2\pi i} \log(z - z_n) - \frac{\Gamma_n \dot{z}_n}{2\pi i (z - z_n)} + \text{conjugate} \right) dz$$

$$= \frac{i\rho}{2} \oint_C \left(2\Re \left[\frac{\dot{\Gamma}_n}{2\pi i} \log(z - z_n) \right] - \frac{\Gamma_n \dot{z}_n}{2\pi i (z - z_n)} \right) dz \tag{1.16}$$

$$= \frac{i\rho \dot{\Gamma}_n}{2\pi} \oint_C \Re[-i \log(z - z_n)] dz - \frac{i\rho \Gamma_n \dot{z}_n}{2},$$

where a dot represents differentiation with respect to time. Now, let C be comprised of the three contours shown in figure (1.2), which are parameterised as follows:

$$\begin{array}{llll}
C_1: & z = z_{n_0} + r e^{i\alpha}: & r \in [0, |z_n - z_{n_0}|] \\
C_2: & z = z_n + \epsilon e^{i\theta}: & \theta \in [0, 2\pi] \\
C_3: & z = z_{n_0} + r e^{i(\alpha + 2\pi)}: & r \in [|z_n - z_{n_0}|, 0]
\end{array} \tag{1.17}$$

where C_3 must be parameterised with angle $\alpha + 2\pi$ since we are going around a branch cut. If we take the limit as $\epsilon \to 0$, and use the Cauchy integral formula for a closed contour containing z_0,

$$f^{(n)}(z_0) = \frac{1}{2\pi n!} \oint \frac{f(z)}{(z - z_0)^{n+1}} \, dz, \tag{1.18}$$

along with the fact that very close to z_n, the contour velocity w_c is roughly the speed of the vortex itself $\dot{z}_n$, we can determine the various components of a by considering

the contours which comprise C, since

$$\oint_C = \oint_{C_1} + \oint_{C_2} + \oint_{C_3}.$$ (1.19)

Firstly, for C_1, we find,

$$\lim_{\epsilon \to 0} \oint_{C_1} 2\Re \left[\frac{\dot{\Gamma}_n}{2\pi i} \log (z - z_n) \right] dz$$

$$= \frac{\dot{\Gamma}_n}{\pi} \int_0^{|z_n - z_{n_0}|} \arg \left((r - |z_n - z_{n_0}|) e^{i\alpha} \right) e^{i\alpha} \, dr$$ (1.20)

$$= \frac{\dot{\Gamma}_n}{\pi} \alpha (z_n - z_{n_0}).$$

For C_2, we get

$$\lim_{\epsilon \to 0} \oint_{C_2} = \frac{\dot{\Gamma}_n}{\pi} \lim_{\epsilon \to 0} \int_0^{2\pi} \arg \left(\epsilon e^{i\theta} \right) i\epsilon \, d\theta = 0.$$ (1.21)

Similarly to C_1, we find the integral along C_3 to be

$$\lim_{\epsilon \to 0} \oint_{C_3} = -\frac{\dot{\Gamma}_n}{\pi} (2\pi + \alpha) (z_n - z_{n_0}).$$ (1.22)

Therefore, we find

$$a = -\frac{i\rho}{2} \Gamma_n \dot{z}_n - i\rho \dot{\Gamma}_n (z_n - z_{n_0}).$$ (1.23)

We find that $b = 0$ because $\bar{w} = -\frac{\Gamma_n}{2\pi i (\bar{z} - \bar{z}_n)} + \bar{\tilde{w}}$ is analytic inside C. Now, let's consider integral c,

$$c = - \overline{\left(\frac{i\rho}{2} \oint_C w^2 \, dz - \frac{i\rho}{2} w_c \oint_C w \, dz \right)}.$$ (1.24)

However, we know by (1.18) that any square terms of w^2 will integrate to give zero so we are left with,

$$c = - \overline{\left(\frac{i\rho}{2} \oint_C \frac{2\tilde{w}_n \Gamma_n}{2\pi i (z - z_n)} \, dz - \frac{i\rho}{2} w_c \Gamma_n \right)}$$

$$= i\rho \bar{\tilde{w}}_n \Gamma_n - \frac{i\rho}{2} \dot{z}_n \Gamma_n.$$ (1.25)

Therefore, (1.13) gives,

$$- i\rho \left(\dot{z}_n \Gamma_n + \dot{\Gamma}_n (z_n - z_{n_0}) - \bar{\tilde{w}}_n \Gamma_n \right) = 0,$$ (1.26)

or, taking the complex conjugate,

$$\frac{d\bar{z}_n}{dt} + \frac{1}{\Gamma_n} \frac{d\Gamma_n}{dt} (\bar{z}_n - \bar{z}_{n_0}) = \tilde{w}_n.$$ (1.27)

14

Where in fact,

$$\tilde{w}_n = w - \frac{\Gamma_n}{2\pi i \left(z_n - z_{n_0}\right)} = \lim_{z \to z_n} \frac{d}{dz} \left[F - \frac{\Gamma_n}{2\pi i} \log \left(z - z_n\right) \right]. \tag{1.28}$$

Now, if we let the vortex have circulation of the opposite sign, $\hat{\Gamma}_n = -\Gamma_n$, which makes no difference since the sign of Γ_n is arbitrary, we arrive at the final equation of motion,

$$\frac{d\bar{z}_n}{dt} + \frac{1}{\hat{\Gamma}_n} \frac{d\hat{\Gamma}_n}{dt} \left(\bar{z}_n - \bar{z}_{n_0}\right) = \lim_{z \to z_n} \frac{d}{dz} \left[F - \frac{i\hat{\Gamma}_n}{2\pi} \log \left(z - z_n\right) \right], \tag{1.29}$$

which henceforth I will refer to as the Brown-Michael Equation.

It should also be noted that the equation of motion for a vortex at z_j, with constant circulation Γ_j is given by taking the limit of the derivative of the complex velocity potential without the vortex itself, which is identically $\tilde{w}_j$:

$$\frac{d\bar{z}_j}{dt} = u_j - iv_j = \lim_{z \to z_j} \frac{d}{dz} \left(F - \frac{i\Gamma_j}{2\pi} \log \left(z - z_j\right) \right). \tag{1.30}$$

In the Brown-Michael model, the point vortex is given circulation which depends on time and this dependence gives rise to an extra term in the equation of motion.

Chapter 2

Flow without the Kutta Condition

In this chapter, we will neglect the Brown-Michael model and investigate vortex trajectories using Hamiltonian dynamics.

2.1   Gap in a Wall

Johnson and McDonald (2004) investigated the case of a gap in an infinitely long wall. This domain consists of one solid boundary at $\Im z = 0, \Re z \leq 1$ and another at $\Im z = 0, \Re z \geq 1$. We will make the following conformal map from the upper half of the mathematical ζ-plane to the physical z plane:

$$z = \frac{1}{2}\left(\zeta + \frac{1}{\zeta}\right), \quad \zeta = z + \left(z^2 - 1\right)^{1/2}, \tag{2.1}$$

where we choose the branch of the square root that has positive imaginary part. The gap in the z-plane maps to the unit semicircle in the upper half of the ζ-plane, while the boundaries map to the line $\Im\zeta = 0$. To help envisage the form of the Hamiltonian (1.1) for N vortices in the ζ-plane, let us first take the simple case of two vortices at positions ζ_1 and ζ_2, with strengths Γ_1 and Γ_2, respectively. There are two image vortices located at $\bar{\zeta}_1$ and $\bar{\zeta}_2$ with strengths $-\Gamma_1$ and $-\Gamma_2$ respectively. The streamfunction for this flow at ζ_1 is:

$$\begin{aligned}
\psi\left(\zeta_1\right) &= -\frac{\Gamma_2}{4\pi}\log\left|\frac{\zeta_1 - \zeta_2}{\zeta_1 - \bar{\zeta}_2}\right| + \frac{\Gamma_1}{4\pi}\log\left|\zeta_1 - \bar{\zeta}_1\right| \\
&= \Gamma_2 G\left(\zeta_1, \zeta_2\right) + \Gamma_1 G_H^{(1)}\left(\zeta_1\right).
\end{aligned} \tag{2.2}$$

Given the apparent form of the Greens functions, we can write down the Hamiltonian for a system of N vortices using (1.1),

$$H\left(\zeta_1, \ldots \zeta_N\right) = -\frac{1}{4\pi}\sum_{i \neq j}^{N}\Gamma_i\Gamma_j\log\left|\frac{\zeta_i - \zeta_j}{\zeta_i - \bar{\zeta}_j}\right| + \frac{1}{4\pi}\sum_{i=1}^{N}\Gamma_i^2\log\left|2\Im\zeta_i\right|. \tag{2.3}$$
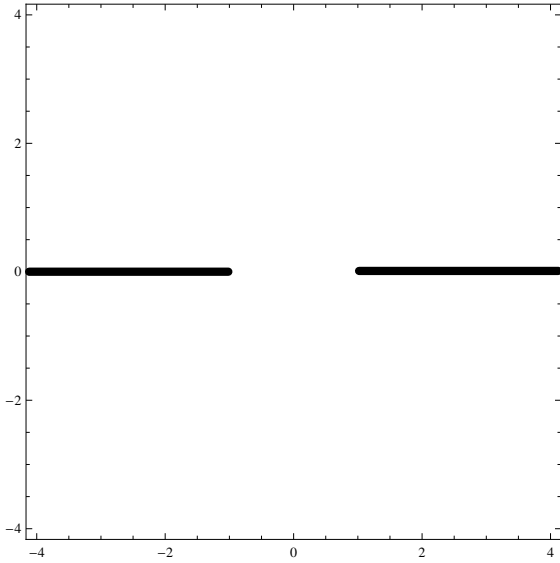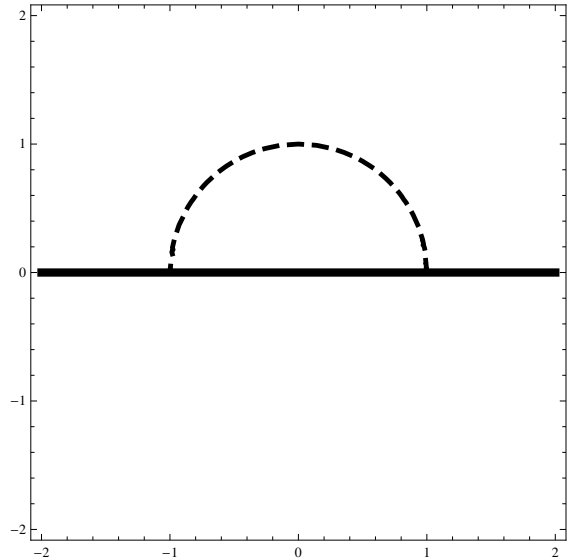
Figure 2.1: z-plane

Figure 2.2: ζ-plane, where the dashed line represents the gap under the mapping

We know the derivative of the conformal map, $F'(\zeta) = \frac{1}{2}\left(1 - \zeta^{-2}\right)$, and so, from (1.6), the Hamiltonian in the physical plane is,

$$H\left(z_1, \ldots z_N\right) = -\frac{1}{4\pi}\sum_{i \neq j}^{N}\Gamma_i\Gamma_j \log\left|\frac{\zeta_i - \zeta_j}{\zeta_i - \bar{\zeta}_j}\right| + \frac{1}{4\pi}\sum_{i=1}^{N}\Gamma_i^2 \log\left|\Im\zeta_i\left(1 - \zeta_i^{-2}\right)\right|. \qquad (2.4)$$

In the case $N = 1$, the Hamiltonian is also the Kirchoff-Routh path function. It is so called because at constant values it gives the vortex trajectories. In this case, the first term of (2.4) is zero, and therefore the trajectories of this vortex are given by,

$$\left|\Im\zeta\left(1 - \zeta^{-2}\right)\right| = \text{const.} \qquad (2.5)$$

As we take the limit $\zeta \to \infty$,

$$\zeta \to x_\infty + iy_\infty + \left(\left(x_\infty + iy_\infty\right)^2 - 1\right)^{\frac{1}{2}} \to 2\left(x_\infty + iy_\infty\right), \qquad (2.6)$$

and therefore,

$$\left|\Im\zeta\left(1 - \zeta^{-2}\right)\right| \to 2y_\infty. \qquad (2.7)$$

As seen in figure (2.3), the dividing trajectory, also called the separatrix, which defines whether the vortices skim over the gap or pass through it goes through the origin of the z-plane $z = 0 \to \zeta = i$. Therefore $y_\infty = \pm 1$, implying that if the vortex begins closer than half of the distance of the gap from the barrier, then it will pass through. Otherwise, it will skim across it.
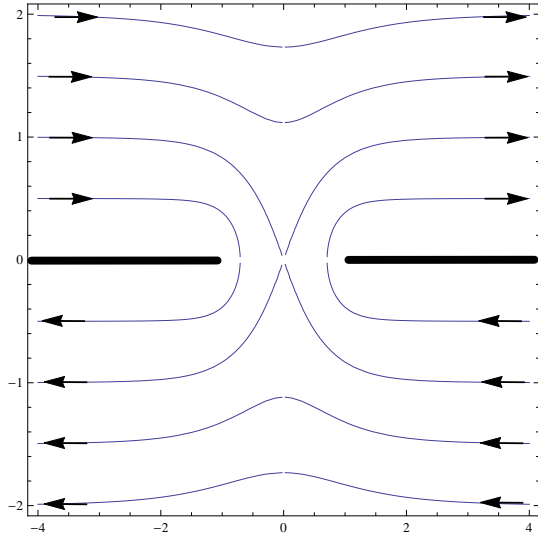
Figure 2.3: Vortex trajectories for various initial conditions without background flow.
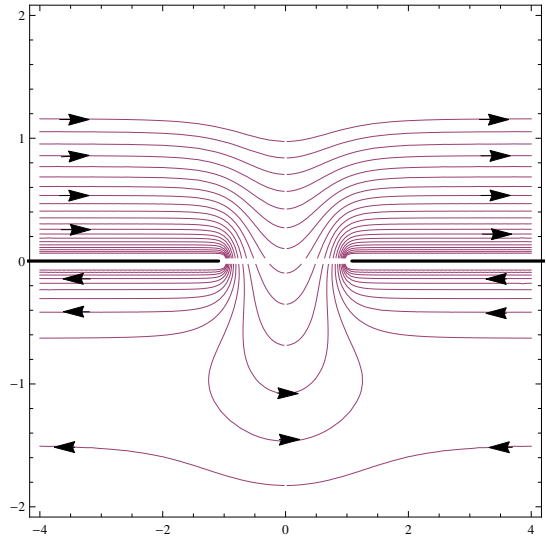

Figure 2.4: Superimposing a uniform stream in the positive x direction, $\alpha = 1$, we drive vortices which start in the upper half plane across the gap, whereas the ones which slip through are pushed backwards.
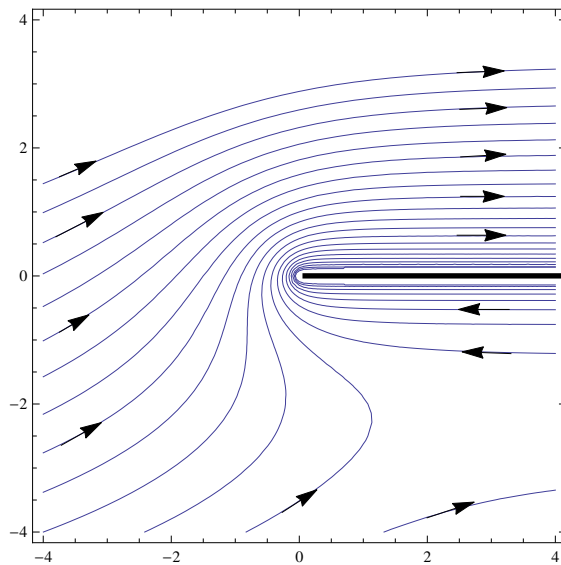

Figure 2.5: Vortex trajectories for various initial conditions near a single sharp edge with a uniform flow $\alpha = 1$.

2.2 Background Flow

Let us now consider a background flow superimposed on the current model with complex velocity potential,

$$F(z) = \alpha z. \tag{2.8}$$

This corresponds to a uniform stream of strength α in the positive x-direction, where $z = x + iy$. The Hamiltonian for this background flow is,

$$H = \sum_{i=1}^{N} \Gamma_i \psi(z_i) = \sum_{i=1}^{N} \Gamma_i \Im(F(z_i)), \tag{2.9}$$

so for the entire system we have,

$$H(z_1, \ldots z_n) = -\frac{1}{4\pi} \sum_{i \neq j}^{N} \Gamma_i \Gamma_j \log \left| \frac{\zeta_i - \zeta_j}{\zeta_i - \bar{\zeta}_j} \right| + \frac{1}{4\pi} \sum_{i=1}^{N} \Gamma_i^2 \log \left| \Im \zeta_i \left(1 - \zeta_i^{-2} \right) \right|$$

$$+ \sum_{i=1}^{N} \Gamma_i \alpha y. \tag{2.10}$$

Or in the $N = 1$ case,

$$H(z) = \frac{1}{4\pi} \Gamma^2 \log \left| \Im \zeta \left(1 - \zeta^{-2} \right) \right| + \Gamma \alpha y. \tag{2.11}$$

We find the vortex trajectories at lines of constant H and the results can be seen in in figure (2.4).

2.3 Near the Edge

Now let us examine the flow very close to the edge of one of the walls, and we will choose the right hand wall without loss of generality. It is sufficient to consider this barrier alone, ignoring the interference of the other because at sufficiently close distances to the right wall, the effect of the left wall is negligible. The domain is therefore the z-plane with a single solid barrier at $\Re z > 0, \Im z = 0$. A suitable conformal map from the mathematical plane is

$$\zeta = \sqrt{z}. \tag{2.12}$$

The Hamiltonian is therefore,

$$H(z_1, \ldots z_n) = -\frac{1}{4\pi} \sum_{i \neq j}^{N} \Gamma_i \Gamma_j \log \left| \frac{\sqrt{z_i} - \sqrt{z_j}}{\sqrt{z_i} - \sqrt{\bar{z}_j}} \right| + \frac{1}{4\pi} \sum_{i=1}^{N} \Gamma_i^2 \log |4 \sqrt{z_i} \Im \sqrt{z_i}|, \tag{2.13}$$

or in the $N = 1$ case,

$$H\left(z\right) = \frac{1}{4\pi}\Gamma^2 \log\left|4\sqrt{z}\Im\sqrt{z}\right| = \Gamma\psi\left(z\right). \tag{2.14}$$

Therefore, if we let $z = re^{i\theta}$, from (1.7) the streamfunction is

$$\begin{aligned}
\psi\left(z\right) &= \frac{\Gamma}{8\pi}\log\left|\sqrt{z}\Im\sqrt{z}\right|^2 + C \\
&= \frac{\Gamma}{8\pi}\log\left|\sqrt{r}\left(\sqrt{r}\sin\frac{\theta}{2}\right)\right|^2 + C \\
&= \frac{\Gamma}{8\pi}\log\frac{r^2}{2}\left(1 - \cos\theta\right) + C \\
&= \frac{\Gamma}{8\pi}\log\left(x^2 + y^2 - x\left(x^2 + y^2\right)^{1/2}\right) + A,
\end{aligned} \tag{2.15}$$

where A and C are constants. Superimposing the background uniform flow with $\alpha = 1$, and altering the dimensions x and y appropriately, we find the vortex trajectories at lines of constant

$$\psi_o = y + \log\left(x^2 + y^2 - x\left(x^2 + y^2\right)^{1/2}\right). \tag{2.16}$$

We can see the results in figure (2.5).

Several variations of the vortex near a sharp edge problem have now been investigated, however, we have completely ignored a very important complication which is fundamental to this problem. The behaviour of the fluid near to the edge itself is problematic because the velocity field for the flow becomes singular at the plate tips. Therefore, we must introduce a new model altogether, imposing the Kutta condition at the tips and solving the Brown-Michael equation for the vortex positions.

Chapter 3

Separated Flow past a Semi-Infinite Plate

Here we will look at a variety of flow cases past a semi-infinite plate using the Brown-Michael model (1954).

3.1 Cortelezzi Problem

First, following the method of Cortelezzi, we will explore the effects of an unsteady flow $U(t)$ past the plate. The boundary will be represented by $\Im z = 0, \Re z < 0$. We use the Brown-Michael model for the viscous effect of a separated boundary layer which rolls up into a spiral. A point vortex will represent the spiral and will be connected to the tip by a vortex sheet of negligible width. The vortex will change position and circulation over time due to its being continuously fed vorticity by the tip.

3.1.1 Conformal Map, Equations of Motion and Exact Solution

The conformal map from the upper half, or mathematical ζ-plane, to the physical plane, $z = -\zeta^2, \quad \zeta = i\sqrt{z}$, allows us to find the complex velocity potential in the
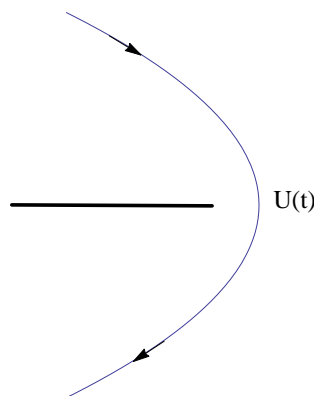
U(t)

Figure 3.1: Unsteady flow past a semi-infinite plate in the physical z-plane

ζ-plane using the method of images,

$$F(\zeta, t) = U(t)\zeta + \frac{i\Gamma(t)}{2\pi} \log \frac{\zeta - \zeta_1(t)}{\zeta - \bar{\zeta}_1(t)}, \tag{3.1}$$

where ζ_1 is the position of the shed vortex with circulation $\Gamma(t)$, and $\bar{\zeta}_1$ represents its conjugate position, corresponding to the image vortex in the ζ-plane. The image is necessary so that the impermeability condition $v_n = 0$ on the wall is satisfied, where v_n is the velocity in the normal direction to the wall.

The velocity field for the fluid in the ζ-plane is therefore,

$$u - iv = \frac{dF}{d\zeta} = U(t) + \frac{i\Gamma(t)}{2\pi} \left(\frac{1}{\zeta - \zeta_1(t)} - \frac{1}{\zeta - \bar{\zeta}_1(t)} \right). \tag{3.2}$$

Imposing the Kutta condition at the tip,

$$\frac{dF}{dz} = \frac{dF}{d\zeta} \frac{d\zeta}{dz} = finite, \quad \zeta = z = 0, \tag{3.3}$$

we know that $\frac{d\zeta}{dz} = -\frac{1}{2\zeta} \to \infty, \quad \zeta \to 0$, so we must have $\frac{dF}{d\zeta} = 0, \quad \zeta = 0$. Thus, we can derive a formula for the circulation of the shed vortex using (3.2),

$$\Gamma_1(t) = 2\pi i U(t) \frac{\zeta_1 \bar{\zeta}_1}{\zeta_1 - \bar{\zeta}_1} = \pi U(t) \left(\frac{|\zeta_1|^2}{\Im \zeta_1} \right). \tag{3.4}$$

Letting the vortex begin at the tip of the plate such that $z(0) = 0$ we can rewrite (1.29) for this system in terms of ζ. We find the limit in the right hand side of the equation using L'Hopital's rule and (3.4) and arrive at,

$$\frac{d\bar{\zeta}_1}{dt} - \frac{1}{2}\bar{\zeta}_1 \left(\frac{|\zeta_1|^2}{\Im \zeta_1} \Im \left[\frac{1}{\zeta_1^2} \frac{d\zeta_1}{dt} \right] \right) = -\frac{\dot{U}}{2U}\bar{\zeta}_1 - \frac{U}{4|\zeta_1|^2} \left(1 - \frac{|\zeta_1|^2}{4\Im \zeta_1} \left(\frac{i}{\zeta_1} + \frac{1}{\Im \zeta_1} \right) \right), \tag{3.5}$$

where a dot represents differentiation with respect to time. Converting to polar coordinates, $\zeta_1 = r_1 e^{i\theta_1}, \quad \bar{\zeta}_1 = r_1 e^{-i\theta_1}$, (3.5) becomes

$$\frac{3}{2}\dot{r}_1 - ir_1\dot{\theta}_1 - \frac{1}{2}r_1\dot{\theta}_1 \cot \theta_1 = -\frac{r_1\dot{U}}{2U} + \frac{U}{4r_1^2} \left(e^{i\theta_1} - \frac{1}{4\sin \theta_1} \left(i + \frac{e^{i\theta_1}}{\sin \theta_1} \right) \right). \tag{3.6}$$

We find the real and imaginary parts to be:

$$\begin{array}{ll} \Re : & \frac{3}{2}\dot{r}_1 - \frac{1}{2}r_1\dot{\theta}_1 \cot \theta_1 = -\frac{r_1\dot{U}}{2U} + \frac{U \cos \theta_1}{16r_1^2 \sin^2 \theta_1} (1 - 2\cos 2\theta_1) \\ \Im : & -r_1\dot{\theta}_1 = -\frac{U \cos 2\theta_1}{8r_1^2 \sin \theta_1} \end{array}, \tag{3.7}$$

which give us the equations of motion:

$$\dot{\theta}_1 = \frac{U \cos 2\theta_1}{8r_1^3 \sin \theta_1}, \qquad \dot{r}_1 = \frac{U \cos \theta_1}{12r_1^2} - \frac{r_1\dot{U}}{3U}, \tag{3.8}$$

with initial conditions,

$$r_1(0) = 0, \quad \theta_1(0) = \theta_0 \in (0, \pi), \tag{3.9}$$

since the vortex must start somewhere in the upper half plane. It is observed that (3.8) is a pair of ordinary differential equations which are singular at the initial value of r_1. To solve them, it is necessary to make another change of variables proposed by McLaughlin et al. (1986):

$$\alpha = Ur_1^3, \quad \beta = \cos\theta_1, \quad \tilde{t} = \int_0^t U^2(\hat{t})\, d\hat{t}. \tag{3.10}$$

Then $(3.8 - 3.9)$ become,

$$\frac{d\alpha}{d\tilde{t}} = \frac{\beta}{4}, \quad \frac{d\beta}{d\tilde{t}} = \frac{1 - 2\beta^2}{8\alpha}, \tag{3.11}$$
$$\alpha(0) = 0, \quad \beta(0) = \beta_0 \in (-1, 1).$$

They combine to give,

$$\frac{d^2}{d\tilde{t}^2}(\alpha^2) = \frac{1}{16}, \tag{3.12}$$

and, then we can solve to get,

$$\alpha = \pm\frac{\tilde{t}}{4\sqrt{2}}, \quad \beta = \pm\frac{1}{\sqrt{2}}, \tag{3.13}$$

where $\alpha = Ur_1^3$ is positive or negative depending on the sign of $U(t)$. Furthermore, the sign of β must always match that of α. In polar coordinates,

$$r_1 = \left(\frac{1}{4U\sqrt{2}}\int_0^t U^2(\hat{t})\, d\hat{t}\right)^{\frac{1}{3}}, \tag{3.14}$$

$$\theta_1 = \begin{cases} \frac{\pi}{4} & U > 0, \\ \frac{3\pi}{4} & U < 0, \end{cases} \tag{3.15}$$

and therefore, if we assume $U > 0$,

$$\zeta_1 = \sqrt{i}\left(\frac{1}{4U\sqrt{2}}\int_0^t U^2(\hat{t})\, d\hat{t}\right)^{\frac{1}{3}}. \tag{3.16}$$

Hence, the position of the point vortex in the physical plane is,

$$z_1(t) = -\zeta_1^2 = -i\left(\frac{1}{4U\sqrt{2}}\int_0^t U^2(\hat{t})\, d\hat{t}\right)^{\frac{2}{3}}. \tag{3.17}$$

Clearly z_1 is purely negative and imaginary, meaning that as time progresses, the vortex will move purely in the negative imaginary direction, perpendicular to the plate.

However, if we were to change the sign of U such that α became negative, then we would get,

$$z_1\left(t\right) = i\left(\frac{1}{4U\sqrt{2}}\int_0^t U^2\left(\hat{t}\right)d\hat{t}\right)^{\frac{2}{3}}. \tag{3.18}$$

Consequently the vortex would move purely in the positive imaginary direction, perpendicular to the plate.

3.1.2 Stability

It is of interest to ascertain whether these trajectories are stable. If we let and $\theta_1 = \theta_0 + \xi\left(t\right)$, where $0 < \xi \ll 1$ and θ_0 is either $\frac{\pi}{4}$ or $\frac{3\pi}{4}$ depending on the sign of U, then (3.8) becomes,

$$\dot{\xi} \approx -\frac{\xi|U|\sqrt{2}}{4r_1^3}, \tag{3.19}$$

so ξ decays exponentially with time implying that the trajectories are stable.

3.1.3 Cirulation Analysis

The circulation can now be found from (3.4),

$$\Gamma_1\left(t\right) = \pi U\left(\frac{1}{2U}\int_0^t U^2\left(\hat{t}\right)d\hat{t}\right)^{\frac{1}{3}}, \tag{3.20}$$

and consequently, the rate of circulation,

$$\frac{d\Gamma_1}{dt} = \frac{\pi}{3}U\left(-\frac{\dot{U}}{2U^2}\int_0^t U^2\left(\hat{t}\right)d\hat{t} + \frac{U}{2}\right)\left(\frac{1}{2U}\int_0^t U^2\left(\hat{t}\right)d\hat{t}\right)^{-\frac{2}{3}}$$

$$+\pi\dot{U}\left(\frac{1}{2U}\int_0^t U^2\left(\hat{t}\right)d\hat{t}\right)^{\frac{1}{3}} \tag{3.21}$$

$$= \frac{\pi}{3}U\left(\dot{U}\int_0^t U^2\left(\hat{t}\right)d\hat{t} + \frac{U^3}{2}\right)\left(\frac{U^2}{2}\int_0^t U^2\left(\hat{t}\right)d\hat{t}\right)^{-\frac{2}{3}}.$$

Notice how a change in sign of $\frac{dU}{dt}$ could cause a change of sign in the rate of circulation, which is wholly unphysical because the vortex is being continually fed by the shedding of vorticity at the tip. The Brown-Michael model (1954) imposes the condition that if this should happen at time t_s, then the circulation for that vortex will remain constant $\Gamma_1(t) = \Gamma_1(t_s), \quad \forall t > t_s$ and a new vortex must begin at the tip. Henceforth this will be referred to as a circulation event. Then we get,

$$\frac{dU}{dt}\left(t_s\right) = -\frac{1}{2}U^3\left(t_s\right)\left(\int_0^{t_s} U^2\left(\hat{t}\right)d\hat{t}\right)^{-1}. \tag{3.22}$$

For $t < t_s$, however, the freestream velocity must be a function whose magnitude is monotonically increasing with time for the model to be physically valid. Let us assume that such an event does not take place lest the new vortex-vortex interaction complicate the dynamics, for I will investigate this later. Then our exact solution tells us that a vortex is shed from the tip and moves perpendicular to the plate with circulation increasing in magnitude.

3.1.4 Rescaling

Let us rescale our variables in following manner:

$$\hat{z}_1 = z_1, \quad \hat{t} = \frac{1}{U} \int_0^t U^2 \left(\acute{t}\right) d\acute{t}, \quad \hat{U} = 1, \quad \hat{\Gamma}_1 = \frac{\Gamma_1}{U}, \tag{3.23}$$

such that equations (3.20) and (3.17) become,

$$\hat{\Gamma}_1 = \pi \left(\frac{\hat{t}}{2}\right)^{\frac{1}{3}}, \quad \hat{z}_1 = -i \left(\frac{\hat{t}}{4\sqrt{2}}\right)^{\frac{2}{3}}. \tag{3.24}$$

Then the rate of circulation becomes,

$$\frac{d\hat{\Gamma}_1}{d\hat{t}} = \frac{1}{U^2} \left(\dot{\Gamma}_1 - \frac{\Gamma_1}{U}\dot{U}\right) \left(1 - \frac{1}{U^3}\dot{U} \int_0^t U^2 \left(\acute{t}\right) d\acute{t}\right)^{-1}$$
$$= \frac{\pi}{3 \cdot 2^{\frac{1}{3}} \hat{t}^{\frac{2}{3}}}, \tag{3.25}$$

so our new set of equations are completely independent of U. Notice how $(3.24 - 3.25)$ are equivalent to the case where $U = 1$. Therefore, the solution is universal in the sense that 3.24 is valid for any choice of U, under a suitable rescaling.

3.2 Tide Problem

In this problem we will investigate the case of an oscillating flow $U = \sin t$ past a semi-infinite plate with continuously shed vorticity from the tip. This is not too dissimilar from a periodic tide which moves backwards and forwards past a harbour wall or peninsula, shedding vorticity as it moves. With the same Brown and Micheal point vortex model as before, we find that as long as the circulation of the shed vortex does not reach a stationary point, the vortex will move with the stream away from and perpendicular to the plate. However, a change in the sign of $\frac{d\Gamma_1}{dt}$ will violate the Brown-Michael model, forcing the original vortex to maintain constant circulation and a new one to be generated from the tip of the plate with variable circulation, continuously fed by a vortex sheet of negligible width. If the rate of change of circulation of the second vortex then changes sign, we must repeat the process. Here we will investigate the problem up to five changes of sign, that is, up until there are five vortices and we stop the system when there is a circulation event for the fifth vortex.

3.2.1 Equations of Motion

Given N vortices of strength Γ_i at positions ζ_i with images at $\bar{\zeta}_i$ in the mathematical plane, the complex velocity potential is,

$$F(\zeta, t) = \sin(t)\,\zeta + \sum_{i=1}^{N} \frac{i\Gamma_i}{2\pi} \log\left(\frac{\zeta - \zeta_i}{\zeta - \bar{\zeta}_i}\right), \tag{3.26}$$

where, in this model, only the most recently shed vortex has time-dependance and is found using the Kutta condition at $\zeta = 0$. All other vortices have constant, given circulation. If the i'th vortex is released at time t_i and moves with variable circulation
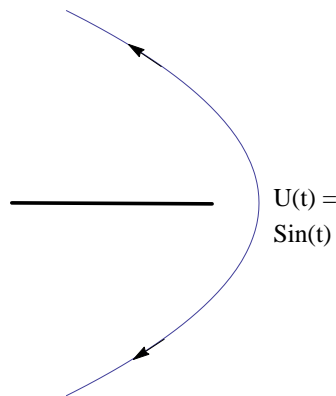

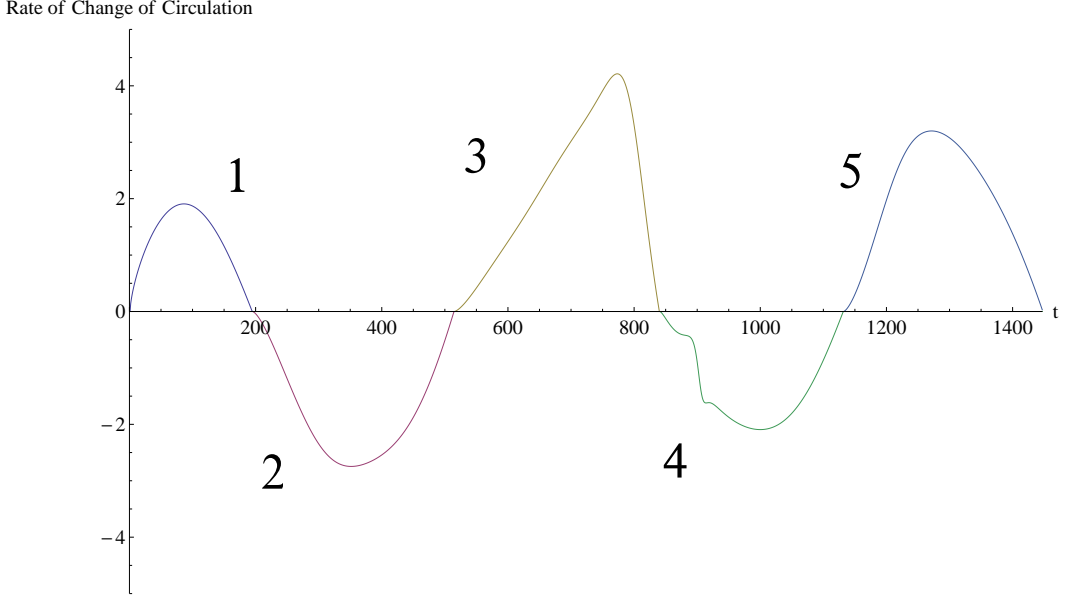Figure 3.2: Physical z-plane depicting an oscillating flow past a semi-infinite plate.

Figure 3.3: Rates of Circulation for consecutive vortices

until time t_s, after which it remains constant, it can be shown that

$$
\Gamma_i(t) = \begin{cases} 0 & t < t_i \\ \frac{\pi |z_i|^2}{\Im z_i}\left(\sin t - \sum_{j=1}^{i-1} \frac{\Gamma_j \Im z_j}{\pi |z_j|^2}\right) & t_i \le t \le t_s \\ \Gamma_i(t_s) & t > t_s \end{cases} \tag{3.27}
$$

The corresponding rate of change of circulation can be shown to be

$$
\frac{d\Gamma_1}{dt} = \begin{cases} 0 & t < t_i \\ 4\pi \left(\frac{1}{\bar{\zeta}_i} - \frac{1}{\zeta_i}\right)^{-2} \Im\left[\frac{1}{\zeta_i^2}\frac{d\zeta_i}{dt}\right]\left(\sin t - \sum_{j=1}^{i-1}\frac{\Gamma_j \Im z_j}{\pi |z_j|^2}\right) & \\ +\frac{\pi |z_i|^2}{\Im z_i}\left(\cos t - \sum_{j=1}^{i-1}\frac{\Gamma_j}{\pi}\Im\left[\frac{1}{z_j^2}\frac{dz_j}{dt}\right]\right) & t_i \le t \le t_s \\ \\ 0 & t > t_s \end{cases} \tag{3.28}
$$

We use (1.29) with initial position $z_{i_0} = \zeta_{i_0} = 0$ for a vortex with variable circulation and (1.30) for a vortex with constant circulation. Hence, at any point in time when there are k vortices in the fluid, we have one differential equation of the form of (1.29) and $k-1$ differential equations of the form (1.30). If each vortex has position $\zeta_i = \xi_i + i\eta_i$, then we can split each differential equation into real and imaginary parts, yielding $2k$ equations for $2k$ unknowns $(\xi_1, \ldots, \xi_k, \eta_1, \ldots, \eta_k)$.
We solve these coupled equations numerically until they break down at a certain time due to a circulation event for the most recently shed vortex. Then we solve the next set of equations with the initial conditions for the existing vortices as their terminal conditions in the former setting. This continues for as long as we like and in fact, a
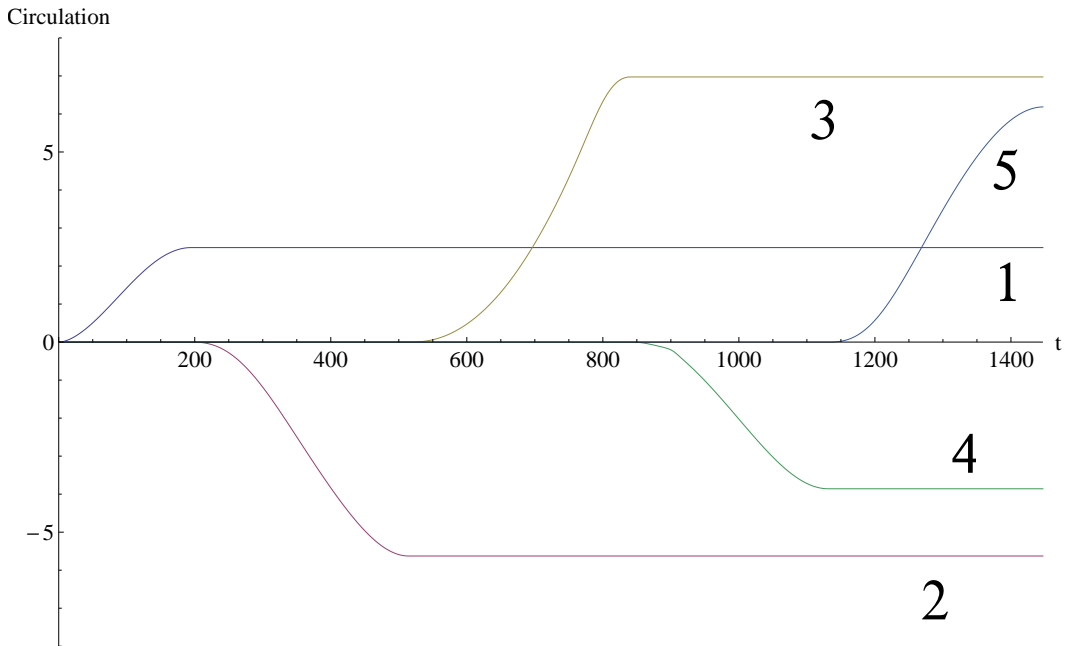
Figure 3.4: Circulations of consecutive vortices

new vortex is shed within every period of the oscillation of the flow $U = \sin t$.

figure (3.3) shows the evolution of the rates of circulation for each consecutive vortex, whereas figure (3.4) depicts the circulations themselves. It is interesting to note that while the sign of the circulation of consecutive vortices alternates, their strengths are not in monotone sequence. The numerical solution gives us the trajectories of the vortices in the mathematical plane but these trajectories are of course no use to us. However, it is possible to map the numerical solution back to the physical z-plane, where $z_i = x_i + iy_i$ using the transform,

$$x_i = -\eta_i^2 + \xi_i^2, \quad y_i = -2\eta_i\xi_i, \tag{3.29}$$

The results can be seen in figure (3.5). The vortices behave quite unexpectedly, pairing up with each other in turn like partners in a waltz. At first, when U is positive and increasing, the first vortex departs from the tip and moves downwards perpendicular to the plate, like in the Cortelezzi problem (1995). After a while a circulation event occurs such that the first vortex henceforth maintains strength of $\Gamma_1 \approx 2.49$ and a second vortex deploys from the tip with circulation of opposite sign to the first. Together they form a dipole and propagate away from the tip until the second vortex has a circulation event. Then the second vortex has constant value $\Gamma_2 \approx -5.63$ of greater magnitude than the first and overpowers it such that they veer off to the left as a pair. In the meantime, a third vortex is released with positive increasing circulation. Eventually it experiences a circulation event and remains at strength $\Gamma_3 \approx 6.97$ thereafter. As a
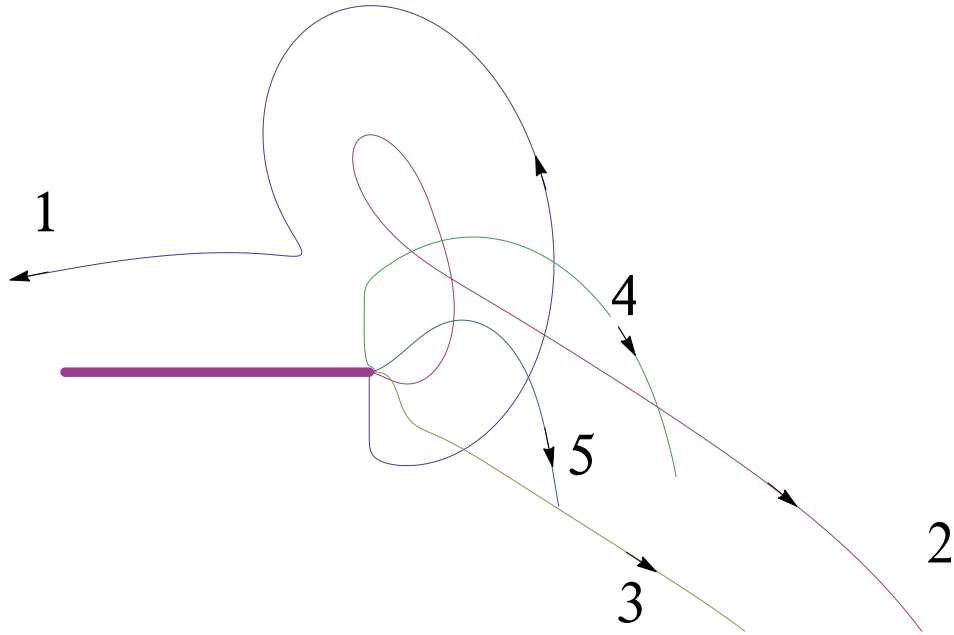
Figure 3.5: Vortex trajectories for the Brown-Michael model (1954) of an oscillating flow past a semi-infinite plate.

consequence of the deployment of a fourth vortex from the tip, the first and second vortex split up such that the first vortex begins to feel the boundary and, appearing to pair up with its image, it travels along the wall in the left direction. The second vortex, having opposite sign and comparable strength to the third, leaves the partnership of the first and pairs up with the third. Seemingly permanent partners, they propagate away from the tip as a dipole. However, their path is slightly askew in favour of the third, owing to the its strength having slightly greater magnitude. After a time, the fourth vortex experiences a circulation event at circulation $\Gamma_4 \approx -3.86$ and a fifth vortex with positive circulation sets out from the tip. All other vortices are quite far away from the tip now such that the fourth and fifth are left undisturbed to pair up as a dipole propagating downwards in favour of the fourth, since they have opposite signs and the fifth is slightly weaker, though growing in strength. This most recent scenario is very similar to the first scenario, when the first and second vortices paired up. This is not too surprising because at the introduction of the fifth vortex, the sign of U is negative and all other vortices are reasonably far away such that the system is not too dissimilar from the original tide problem, except with $U(t) = -\sin t$.

3.2.2 Stability

As with Cortelezzi's example, the ordinary differential equations for the positions of these vortices are all singular at the tip of the plate where all the solutions begin. Unlike before, we cannot make a suitable change of variables to absolve the singularity.

Instead, we alter the initial position of the vortex ever so slightly from $\zeta_1(0) = 0$ to $\zeta_1(0) = 0 + 0.001i$. To ascertain whether these solutions are stable, we can perturb the initial position to $\zeta_1(0) = 0 + 0.0005i$ and $\zeta_1(0) = 0 + 0.002i$. The three results can be seen in figure (3.6) to converge fairly rapidly to the same trajectory. Therefore the supposed initial condition $\zeta_1(0) = 0 + 0.01i$ seems fairly stable and therefore a satisfactory approximation.
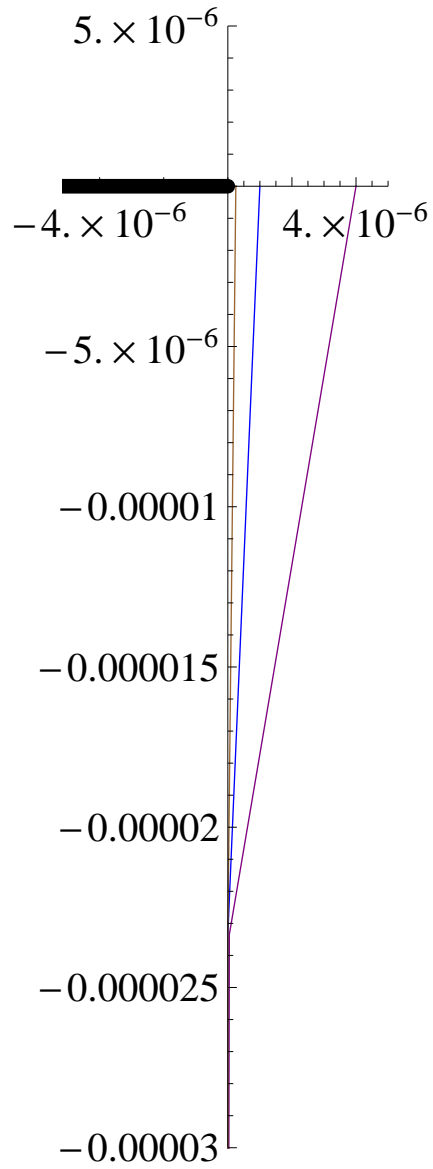
Figure 3.6: Here we witness the convergence of three trajectories in the physical plane for the first vortex of the tide problem. Each trajectory is calculated numerically with different initial conditions, $\zeta_1(0) = 0 + 0.001i, 0 + 0.002i, 0 + 0.0005i$.

3.3 Starting Vortex

Here, in place of a flow past as semi-infinite plate, we investigate the flow driven by a vortex initiated at $z = -\infty + i$ with fixed circulation. Very far away from the tip the vortex will be driven by its image and will propagate parallel to the plate. It is of great interest to understand when the effects of the tip of the plate begin to take place. In other words, we wish to know when the vortex ceases to feel an infinite wall and begins to feel a sharp edge. Then we will ascertain the fate of the vortex after it encounters the tip.

Without imposing the Kutta condition, a vortex at z_1 with strength $\Gamma = const$ which starts near a semi-infinite plate has equation of motion, (1.30). In the ζ-plane this becomes,

$$\frac{d\bar{\zeta}_1}{dt} = -\frac{\Gamma}{16\pi|\zeta_1|^2}\left(\frac{i}{\zeta_1} + \frac{1}{\Im\zeta_1}\right). \tag{3.30}$$

If $\zeta_1 = \xi_1 + i\eta_1$, We split (3.30) into real and imaginary parts and solve the two differential equations numerically. Mapping the solution back using (3.29), we get the trajectories shown in figure (3.7).

A logical step is to investigate the same problem with the Brown-Michael model. We will look at what happens when a vortex with fixed circulation begins far from a sharp edge using precisely the same domains, notation and conformal map as in the tide problem.

3.3.1 Conformal Map and Equations of Motion

Here we must account for the starting vortex and the consequent Brown-Michael shed vortex. In the mathematical plane, as before, we use the method of images to work out the complex velocity potential,

$$F(\zeta, t) = \frac{i\Gamma_1}{2\pi} \log \frac{\zeta - \zeta_1(t)}{\zeta - \bar{\zeta}_1(t)} + \frac{i\Gamma_2(t)}{2\pi} \log \frac{\zeta - \zeta_2(t)}{\zeta - \bar{\zeta}_2(t)}. \tag{3.31}$$
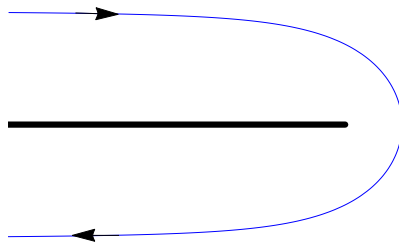

Figure 3.7: Trajectory of vortex near a sharp edge without imposing the Kutta condition.

where ζ_1 and ζ_2 are the positions of the starting vortex and the shed vortex with circulations $\Gamma_1 = -1$ and $\Gamma_2(t)$, respectively, and $\bar{\zeta}_1$ and $\bar{\zeta}_2$ represent the conjugate positions, corresponding to the image vortices in the mathematical plane.

We then find the velocity field to be,

$$\frac{dF}{d\zeta} = u - iv = \frac{i\Gamma_1}{2\pi}\left(\frac{1}{\zeta - \zeta_1} - \frac{1}{\zeta - \bar{\zeta}_1}\right) + \frac{i\Gamma_2(t)}{2\pi}\left(\frac{1}{\zeta - \zeta_2} - \frac{1}{\zeta - \bar{\zeta}_2}\right). \qquad (3.32)$$

Imposing the Kutta condition at the tip, just like before, we find the circulation

$$\Gamma_2(t) = -\Gamma_1\left(\frac{1}{\bar{\zeta}_1} - \frac{1}{\zeta_1}\right)\left(\frac{1}{\bar{\zeta}_2} - \frac{1}{\zeta_2}\right)^{-1} \qquad (3.33)$$
$$= -\Gamma_1\frac{|\zeta_2|^2\Im\zeta_1}{|\zeta_1|^2\Im\zeta_2}.$$

We use Equations (1.29) and (1.30) to find the positions of vortices 1 and 2 respectively. The initial position of the shed vortex is at the tip of the plate, $z_{2_0} = 0$. It is now possible to convert these so that they are in terms of $\zeta_1 = \eta_1 + i\xi_1$ and $\zeta_2 = \eta_2 + i\xi_2$.

$$\frac{d\bar{\zeta}_1}{dt} = \frac{1}{4|\zeta_1|^2}\left(-\frac{i\Gamma_1}{2\pi}\left(\frac{1}{2\zeta_1} + \frac{1}{2i\Im\zeta_1}\right) + \frac{i\Gamma_2}{2\pi}\left(\frac{1}{\zeta_1 - \zeta_2} + \frac{1}{\zeta_1 - \bar{\zeta}_2}\right)\right) \qquad (3.34)$$

$$-2\bar{\zeta}_2\frac{d\bar{\zeta}_2}{dt} - \bar{\zeta}_2^2\left(\Im\left[\frac{1}{\zeta_1^2}\frac{d\zeta_1}{dt}\right]\frac{|\zeta_1|^2}{\Im\zeta_1} - \Im\left[\frac{1}{\zeta_2^2}\frac{d\zeta_2}{dt}\right]\frac{|\zeta_2|^2}{\Im\zeta_2}\right)$$
$$= -\frac{1}{2\zeta_2}\left(\frac{i\Gamma_1}{2\pi}\left(\frac{1}{\zeta_2 - \zeta_1} + \frac{1}{\zeta_2 - \bar{\zeta}_1}\right) - \frac{i\Gamma_2}{2\pi}\left(\frac{1}{2\zeta_2} + \frac{1}{2i\Im\zeta_2}\right)\right). \qquad (3.35)$$

We split these equations into real and imaginary parts, solve numerically for positions in the mathematical plane and map the trajectories back to the physical plane using (3.29). The results can be seen in figure (3.10). From (3.33), we can calculate the variation in circulation of Γ_2 with respect to time, and this together with the circulation itself are plotted in figures (3.8) and (3.9). Comparing figure (3.7) to figure (3.10), we see that the existence of a Brown-Michael vortex drastically alters the path of the vortex. Without the shed vortex, the starting vortex moves parallel to the plate and doesn't 'feel' the sharp edge until it is in close proximity. It then loops around and travels in the reverse direction parallel to the plate. However, in the Brown-Michael model, while the initial path of the starting vortex is similar, when it approaches the tip of the plate it pairs up with the shed vortex, being of opposite sign and comparable strength, and together they form a dipole which shoots off to infinity. Owing to there being no characteristic length scale in this domain, we can deduce that no matter how far above or below we place the starting vortex, it will never pass around the sharp edge.
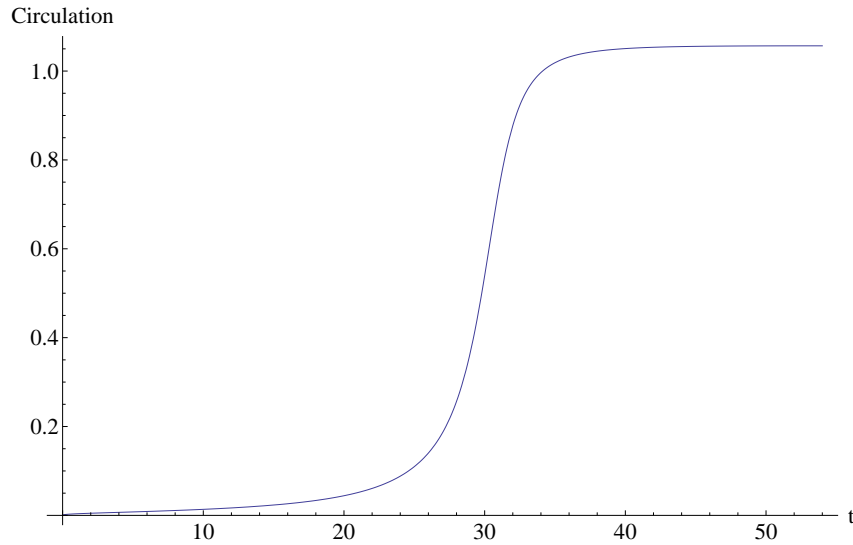
Figure 3.8: Brown-Michael Model: Circulation of the shed vortex.

It should be noted that after a certain amount of time, the shed vortex reaches a peak in its circulation after which it begins to decrease in strength. After this time, we would have to deploy a new vortex from the tip and impose constant circulation on the former, however, the two vortices have already paired up and traveled sufficiently far away that this new vortex has little effect on their paths. We can see this in figure (3.11).

3.3.2   Stability

Similarly to the tide problem, the equation of motion for the shed vortex (3.35) is singular at the tip and so we must replace its initial position with $\zeta_2(0) = 0 + 0.001i$ in the numerical calculation. The stability of the solution can be determined by perturbing the initial position to $\zeta_2(0) = 0 + 0.0005i$ and $\zeta_2(0) = 0 + 0.002i$. As we can see in figure (3.12), the convergence of the three solutions to the same trajectory was rapid, therefore validating the stability of our solution. figure 3.13 shows the result of moving the initial position of the starting vortex double the distance backwards to see if the solutions vary much. Seeing that they do not, it is fair to say that our simulation gives an accurate depiction of the behaviour of a vortex which begins at $z = -\infty + i$.
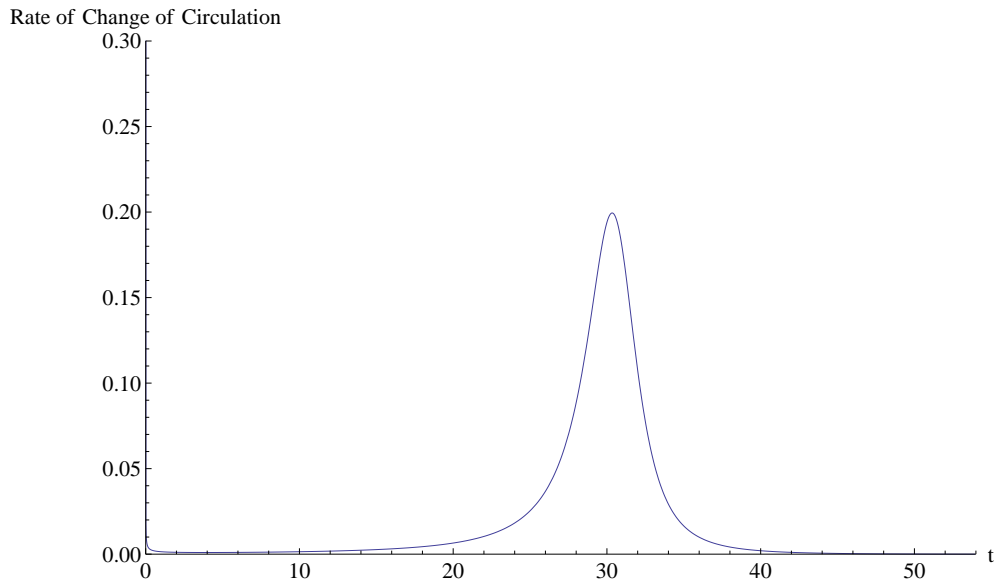
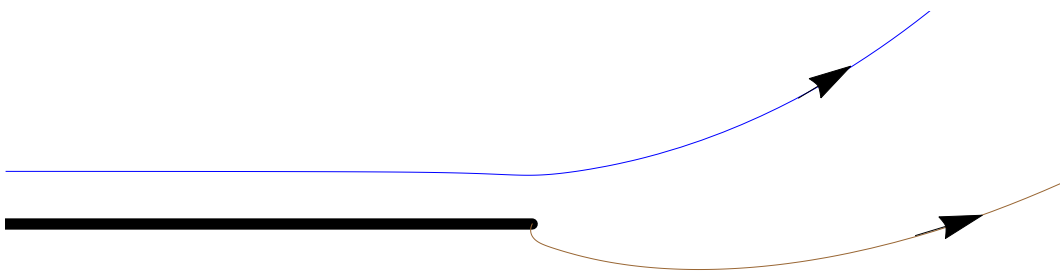Figure 3.9: Brown-Michael Model: Rate of Change of the Circulation of the shed vortex.

Figure 3.10: Brown-Michael Model: Starting Vortex begins at $z = -5 + i$.
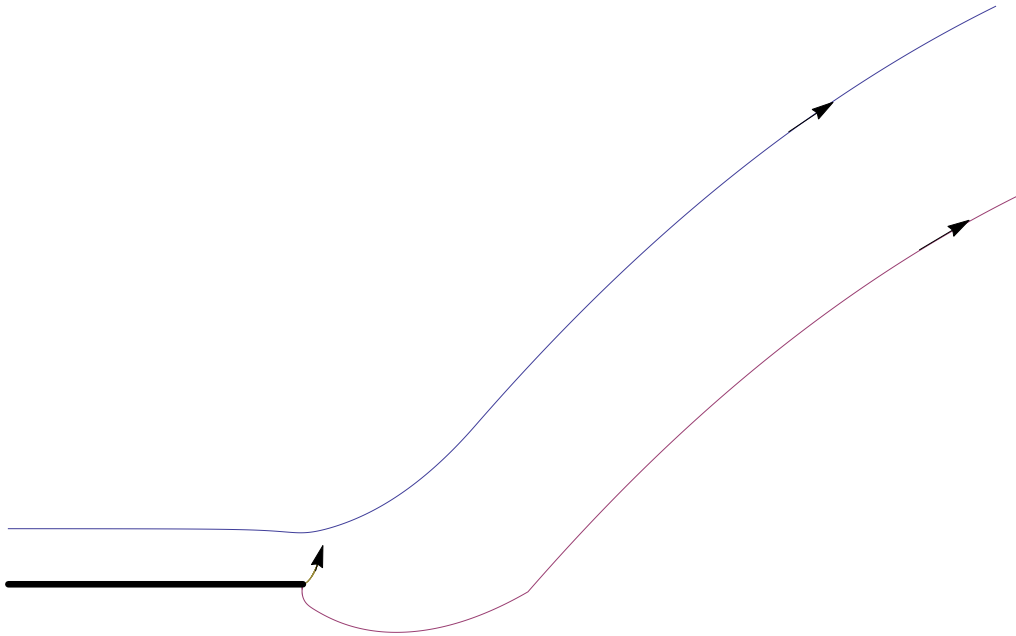
37

Figure 3.11: Prolonged evaluation of the system, where a new vortex is deployed from the tip and the former two travel off barely perturbed to infinity.
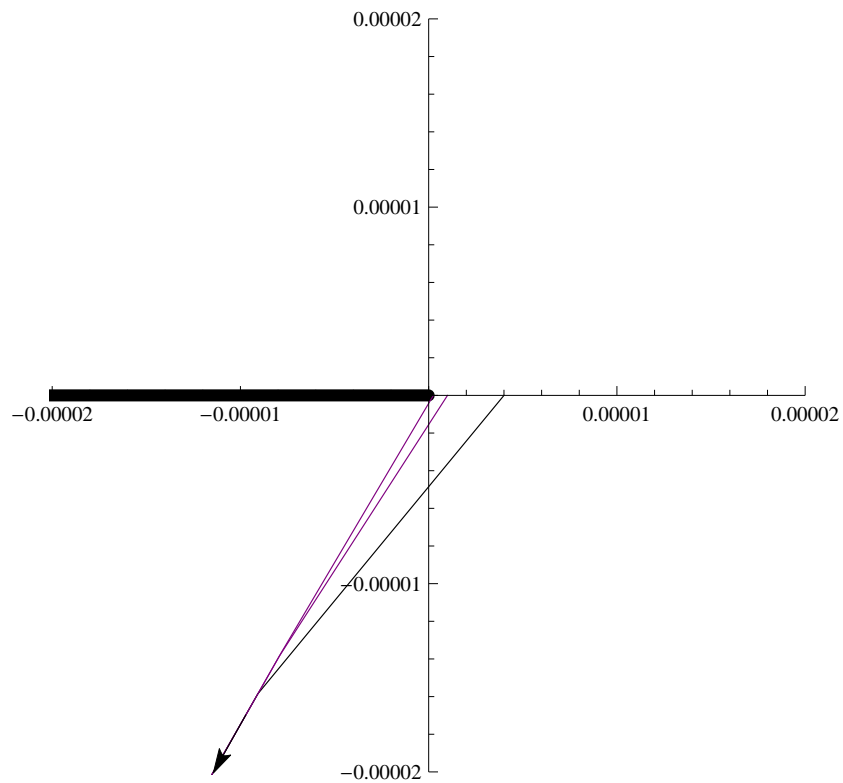

Figure 3.12: Here we witness the convergence of three solutions to the starting vortex problem in the physical plane. The solutions were calculated in the mathematical plane, each with slightly different initial conditions, $\zeta_2(0) = 0 + 0.001i, 0 + 0.002i, 0 + 0.0005i$.
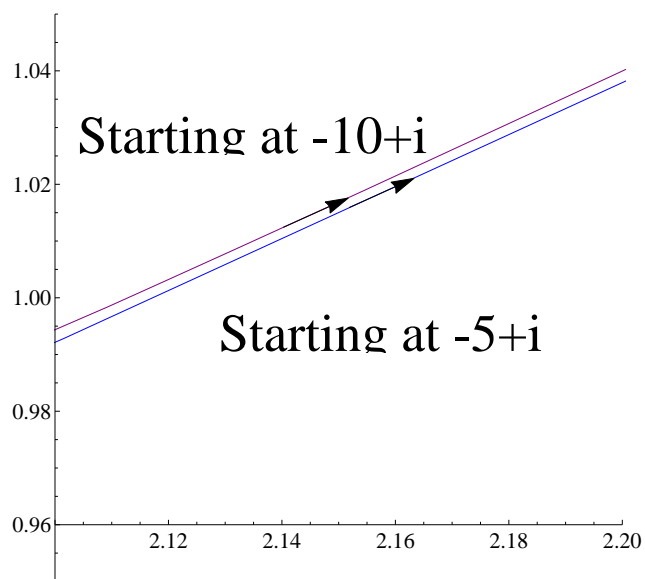
Figure 3.13: Here we see that when the vortex begins even further back at $z = -10 + i$, we can compare its trajectory with that of the original model in which the vortex begins at $z = -5 + i$ and clearly the results are marginally different, being a distance of the order 0.001 apart. Furthermore, the two trajectories appear to be at precisely the same angle. It is obviously impossible to initiate the vortex at $z = -\infty + i$ but it seems that $z = -5 + i$ as approximation to the initial position does not give an inaccurate model.

Chapter 4

Mind the Gap

A logical step would be to revert back to the original case of study, a gap in an infinitely long impermeable wall, and employ the the Brown-Michael model (1954) to a variety of flow cases.

4.1 Separated Steady Flow through the Gap

It is of great interest to investigate the solution to the Brown-Michael equation for a steady flow between two plates so that we can compare the result with Cortelezzi's solution for a flow past a single plate.

4.1.1 Conformal Map and Symmetry

We will use the same conformal map as McDonald and Johnson (2004) to map the physical z-plane with a gap in an infinite plate to the upper half of the mathematical ζ-plane,

$$\zeta = z + \left(z^2 - 1\right)^{\frac{1}{2}}, \quad z = \frac{1}{2}\left(\zeta + \frac{1}{\zeta}\right). \tag{4.1}$$

Introducing a flow through the gap, we acknowledge that by symmetry there will be two vortices shed from the tips of the plates, continuously fed vorticity by vortex sheets of negligible width which connect them to the tips. They have positions $z_1\left(t\right)$ and $z_2\left(t\right)$ with circulations $\Gamma_1\left(t\right)$ and $\Gamma_2\left(t\right)$ respectively. We can exploit an important symmetry property of this problem and reduce its complexity by observing that the two vortices must be images in the line $\Re z = 0$. Therefore it is plain to see that $z_2 = -\bar{z}_1$ and $\Gamma_2 = -\Gamma_1$. It follows that in the ζ-plane,

$$\frac{1}{2}\left(\zeta_2 + \frac{1}{\zeta_2}\right) = -\frac{1}{2}\left(\bar{\zeta}_1 + \frac{1}{\bar{\zeta}_1}\right), \tag{4.2}$$
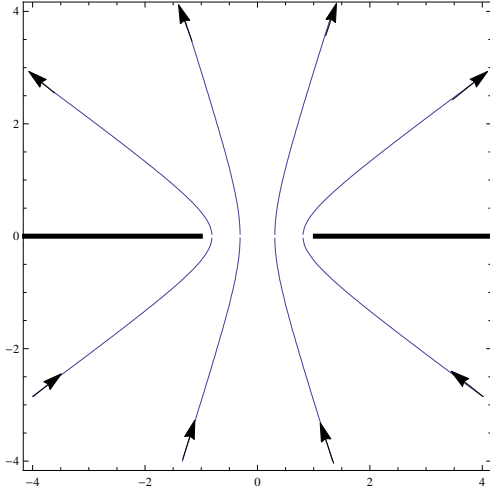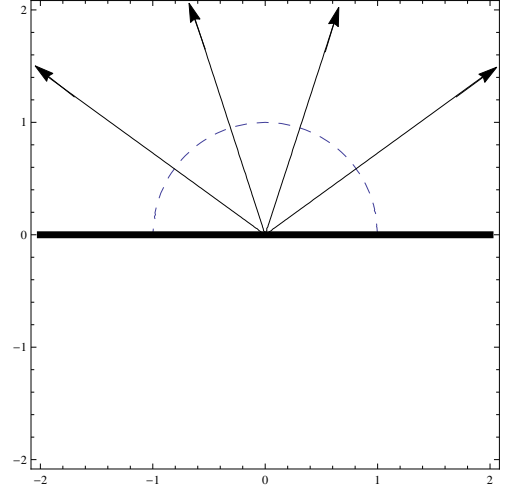
Figure 4.1: z-plane with uniform flow through the gap.

Figure 4.2: Uniform flow through the gap in the ζ-plane where the gap is represented by a dotted semicircle.

which can be seen as a quadratic equation in ζ_2 with solutions,

$$\zeta_2 = -\bar{\zeta}_1, \quad -\frac{1}{\bar{\zeta}_1}. \tag{4.3}$$

However, if we let $\zeta_1 = re^{i\theta}, \quad \theta \in [0, \pi]$, and we choose the second solution then $\zeta_2 = \frac{1}{r}e^{i(\theta+\pi)}$, which is clearly no longer in the upper half of the ζ plane. Therefore we discard this solution and find that $\zeta_2 = -\bar{\zeta}_1$, indicating that in the mathematical ζ-plane, so too are the vortices images in the imaginary axis.

4.1.2 Equations of Motion

In the ζ-plane, we have the complex velocity potential,

$$F\left(\zeta, t\right) = \frac{U}{2\pi} \log \zeta + \frac{i\Gamma_1\left(t\right)}{2\pi} \left(\log \left(\frac{\zeta - \zeta_1}{\zeta - \bar{\zeta}_1} \right) - \log \left(\frac{\zeta + \bar{\zeta}_1}{\zeta + \zeta_1} \right) \right), \tag{4.4}$$

where the first term denotes a source of strength U located at the origin of the ζ-plane, but since the gap in the wall maps to the unit upper semicircle in the ζ-plane, we see in figures (2.1) and (2.2) that this source corresponds to uniform flow through the gap. The second and third terms represent the two vortices at positions ζ_1 and $-\bar{\zeta}_1$ with images at $\bar{\zeta}_1$ and $-\zeta_1$ respectively.

Imposing the Kutta condition at the two tips,

$$\frac{dF}{dz} = \frac{dF}{d\zeta}\frac{d\zeta}{dz} = finite, \quad \zeta = z = \pm 1, \tag{4.5}$$

we know that $\frac{d\zeta}{dz} = \frac{2}{1-\frac{1}{\zeta^2}} \to \infty, \zeta \to \pm 1$, so we must have $\frac{dF}{d\zeta} = 0, \zeta = \pm 1$. Differentiating (4.4) with respect to ζ at $\zeta = \pm 1$, we get the same result, regardless of the choice

of sign,

$$\frac{1}{2\pi} + \frac{i\Gamma_1(t)}{2\pi}\left(\frac{1}{1-\zeta_1} - \frac{1}{1-\bar{\zeta}_1} - \frac{1}{1+\bar{\zeta}_1} + \frac{1}{1+\zeta_1}\right) = 0, \tag{4.6}$$

which yields a formula for the circulation,

$$\Gamma_1(t) = \frac{U|1-\zeta_1^2|^2}{8\Im\zeta_1\Re\zeta_1}. \tag{4.7}$$

We use (1.29) to get our equations of motion and we set $z_{1_0} = -1$ as the initial position of the vortex. In terms of ζ this becomes,

$$\frac{1}{2}\left(1 - \frac{1}{\bar{\zeta}_1^2}\right)\frac{d\bar{\zeta}_1}{dt} - \left(\frac{1}{2}\left(\bar{\zeta}_1 + \frac{1}{\bar{\zeta}_1}\right) + 1\right)\frac{\Im\left(\zeta_1\left(1 - \bar{\zeta}_1^2\right)^2 \frac{d\zeta_1}{dt}\right)}{|1 - \zeta_1^2|^2\Re\zeta_1\Im\zeta_1}$$
$$= \frac{2}{1 - \frac{1}{\bar{\zeta}_1^2}}\left(\frac{U}{2\pi\zeta_1} + \frac{i\Gamma_1}{2\pi}\left(-\frac{1}{2i\Im\zeta_1} - \frac{1}{2\Re\zeta_1} + \frac{1}{2\zeta_1} + \frac{1}{\zeta_1 - \zeta_1^3}\right)\right). \tag{4.8}$$

We can split (4.8) into real and imaginary parts to get two coupled ordinary differential equations for two unknowns, ξ_1 and η_1. Solving numerically, we convert the solutions back to the $z = x + iy$ coordinates using the transform,

$$x = \frac{\xi}{2}\left(1 + \frac{1}{\xi^2 + \eta^2}\right), \tag{4.9}$$

$$y = \frac{\eta}{2}\left(1 - \frac{1}{\xi^2 + \eta^2}\right). \tag{4.10}$$

The trajectories can be seen in figure (4.3), whereas the evolution of the circulation is depicted in figure (4.4). It is noted that Γ_1 and Γ_2 are monotonically decreasing and increasing functions of time respectively. Therefore, our model is valid for all times. The two vortices have opposite signs and equal strengths and therefore pair up as a dipole and propel each other onwards but must have circulation large enough to hold the Kutta condition at the plate tips. That is why we see such a rapid increase in the magnitude of the circulation. The increase is much greater than that in Cortelezzi's semi-infinite plate problem, where $\Gamma_1 \propto t^{\frac{1}{3}}$. Similar to the semi-infinite plate problem, the vortex trajectories are roughly perpendicular to the plate, though slightly perturbed near the beginning. This suggests that it may be possible to find an analytical solution.

4.1.3 Stability

The equation of motion for the vortex (4.8) is singular at of the tip $\zeta = -1$ and so we must replace its initial positions with $\zeta_1(0) = -1 + 0.001i$ in the numerical calculation. The stability of the solution can be determined by perturbing the initial position to
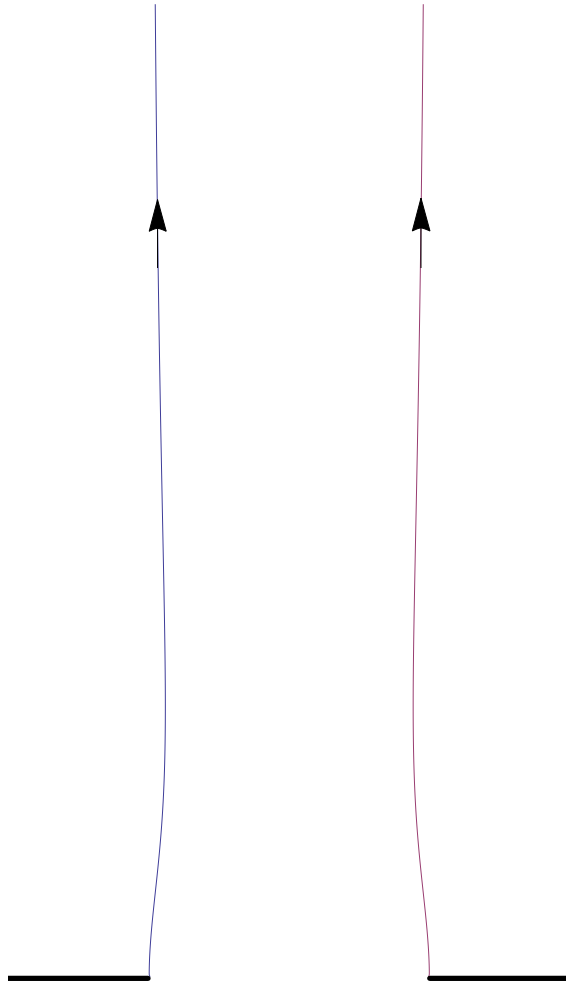
Figure 4.3: Vortex trajectories for a uniform flow $U = 1$ through a gap in an infinitely long wall.
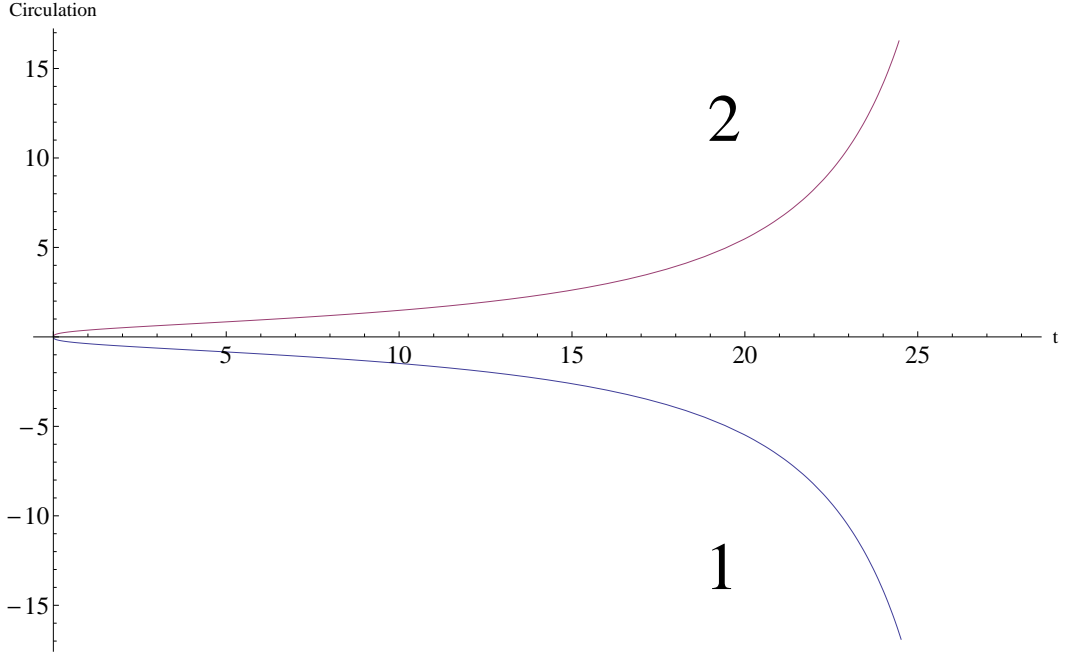
Figure 4.4: Circulations of the two vortices.

$\zeta_1(0) = 0 + 0.0005i$ and $\zeta_1(0) = 0 + 0.002i$. As we can see in figure (4.5), the convergence of the three solutions to the same trajectory was rapid, therefore validating the stability of our solution.

4.1.4 Analytical Solution

It was endeavoured to find an analytical solution to (4.8) by converting to polar coordinates $\zeta_1 = r_1 e^{i\theta_1}$. If we let $P = |1 - \zeta_1^2|^2 = 1 - 2r_1^2 \cos 2\theta_1 + r_1^4$, the resulting equation becomes:

$$
\begin{aligned}
& P^2 \sin 2\theta_1 \left(\dot{r}_1 - ir_1\dot{\theta}_1 \right) \\
& - \left(2r_1^4 + 4ir_1^2 \sin 2\theta_1 - 2 + 4r_1^3 e^{i\theta_1} - 4r_1 e^{-i\theta_1} \right) \\
& \times \left(\dot{r}_1 \sin 2\theta_1 \left(1 - r_1^4 \right) + r_1\dot{\theta}_1 \left(\cos 2\theta_1 \left(1 + r_1^4 \right) - 2r_1^2 \right) \right) \\
& = \frac{U}{\pi} P \left(2r_1^3 \sin 2\theta_1 + \frac{ir_1}{2} - \frac{ir_1^3}{2} e^{-2i\theta_1} + \frac{r_1}{4} P \left(i - e^{i\theta_1} \left(i - e^{i\theta_1} \left(\frac{1}{\sin\theta_1} + \frac{i}{\cos\theta_1} \right) \right) \right) \right)
\end{aligned}
\tag{4.11}
$$

which can be split into real and imaginary parts,

$$
\begin{aligned}
\Re: \quad & \dot{r}_1 \sin 2\theta_1 \left(P^2 + \left(r_1^4 - 1 \right) \left(2 \left(r_1^4 - 1 \right) + 4r_1 \cos\theta_1 \left(r_1^2 - 1 \right) \right) \right) \\
& - r_1\dot{\theta}_1 \left(\cos 2\theta_1 \left(1 + r_1^4 \right) - 2r_1^2 \right) \left(2 \left(r_1^4 - 1 \right) + 4r_1 \cos\theta_1 \left(r_1^2 - 1 \right) \right) \\
& = P \frac{U}{\pi} \left(\frac{3}{2} r_1^3 \sin 2\theta_1 - P \frac{r_1}{2} \cot 2\theta_1 \right),
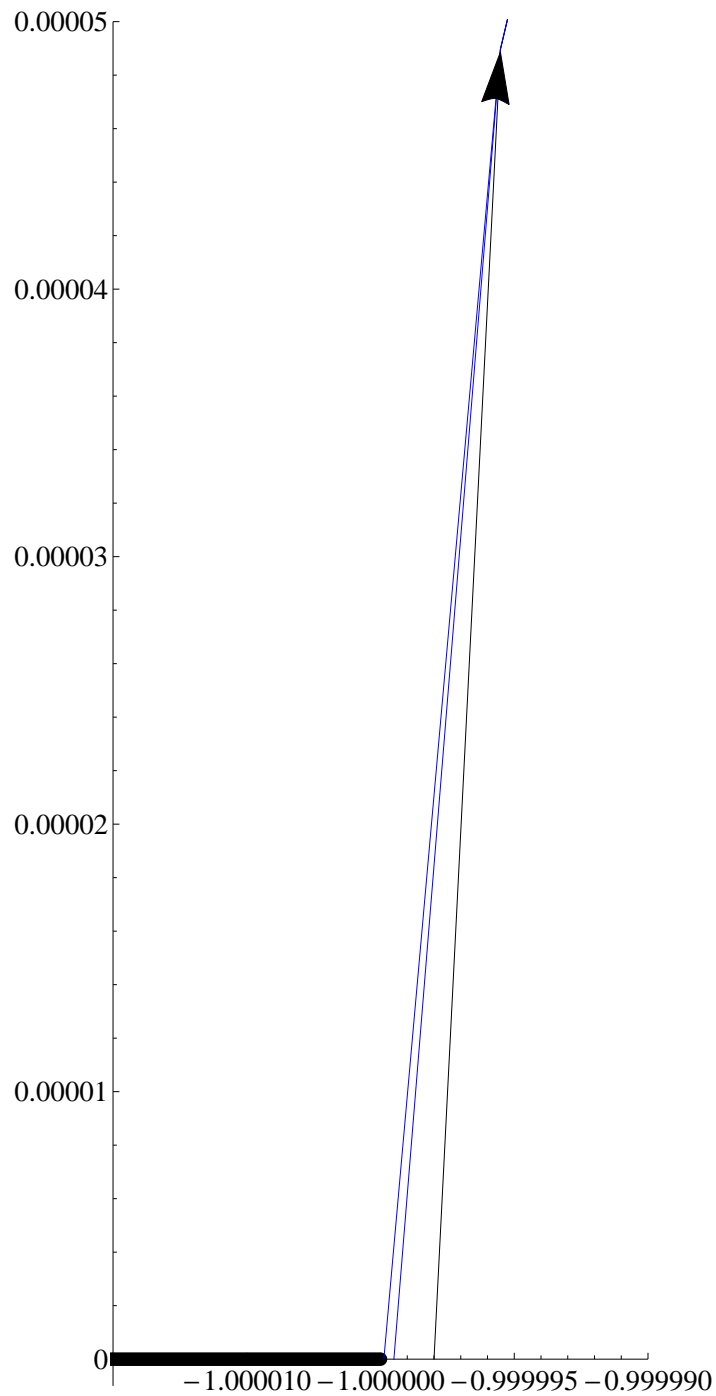\end{aligned}
\tag{4.12}
$$

45

Figure 4.5: Here we witness the convergence of three solutions to the flow through a gap problem in the physical plane. The solutions were calculated in the mathematical plane, each with slightly different initial conditions, $\zeta_1(0) = -1 + 0.001i, -1 + 0.002i, -1 + 0.0005i$. The y-axis has been rescaled by a factor of 0.01 so as to observe the convergence.

$$\Im: \quad 4\dot{r}_1 \sin 2\theta_1 \left(r_1^4 - 1\right) \left(r_1^2 \sin 2\theta_1 + r_1 \sin \theta_1 \left(r_1^2 + 1\right)\right)$$
$$-r_1\dot{\theta}_1 \left(P^2 \sin 2\theta_1 + 4 \left(\cos 2\theta_1 \left(1 + r_1^4\right) - 2r_1^2\right) \left(r_1^2 \sin 2\theta_1 + r_1 \sin \theta_1 \left(r_1^2 + 1\right)\right)\right) \quad (4.13)$$
$$= P\frac{U}{\pi} \left(\frac{r_1}{2} - \frac{r_1^3}{2} \cos 2\theta_1 - \frac{r_1}{4}P\right).$$

After a great deal of painful rearranging, it is unfortunate to say that the attempt was unsuccessful. However, that doesn't go to say that it would be impossible. I encourage anyone brave enough to give it a try.

4.2   Starting Vortex Near the Gap

The next logical step to take is to position a starting vortex with fixed circulation fairly close to the gap and compare the results with figure (2.3). In this model there will be two shed vortices initiating from the tips of the two plates at $z = \pm 1$. We use the conformal map (4.1) and thus, if the starting vortex has position and circulation $\zeta_1(t)$, Γ_1 and the Brown-Michael vortices have positions and circulations $\zeta_2(t)$, $\Gamma_2(t)$ and $\zeta_3(t)$, $\Gamma 3(t)$ where $\zeta_2(0) = -1$ $\zeta_3(0) = 1$ then the complex velocity potential is

$$F(\zeta, t) = F(\zeta, t) = \frac{i\Gamma_1}{2\pi} \log\left(\frac{\zeta - \zeta_1}{\zeta - \bar{\zeta}_1}\right) + \frac{i\Gamma_2}{2\pi} \log\left(\frac{\zeta - \zeta_2}{\zeta - \bar{\zeta}_2}\right) + \frac{i\Gamma_3}{2\pi} \log\left(\frac{\zeta - \zeta_3}{\zeta - \bar{\zeta}_3}\right). \quad (4.14)$$

We are interested in a starting vortex which begins away from the middle of the gap and therefore we lose all symmetry properties. As a Consequence the system becomes extremely complicated and so we solve the entire problem numerically. We use (1.29) for the vortices at positions ζ_1 and ζ_2, and (1.30) for the vortex with constant circulation at ζ_1. To ascertain the functions $\Gamma_2(t)$ and $\Gamma_3(t)$ we solve the pair of simultaneous equations that result from the Kutta condition at $\frac{dF}{d\zeta} = 0$, $\zeta = \pm 1$. To add to the complexity, after a certain amount of time the circulation of the vortex at position ζ_3 reaches a stationary point thereby imposing its then constant value for all future times and initiating a fourth vortex from the tip at $\zeta = z = -1$. In figure (2.3) we saw that a vortex beginning near the gap would slip through if its original vertical distance from the boundary was less than half the width of the gap, and it would otherwise skip over the gap.

However, in figures (4.6) and (4.7), we see that the vortex will skip over if we take its vertical distance as $\frac{1}{20}$ of the width of the gap, which here is 0.1, let alone half.
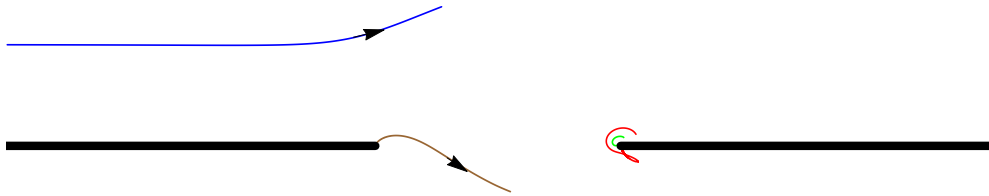
Figure 4.6: Trajectory of a vortex which begins at $z = -4 + i$, along with the trajectories of subsequent Brown-Michael vortices.
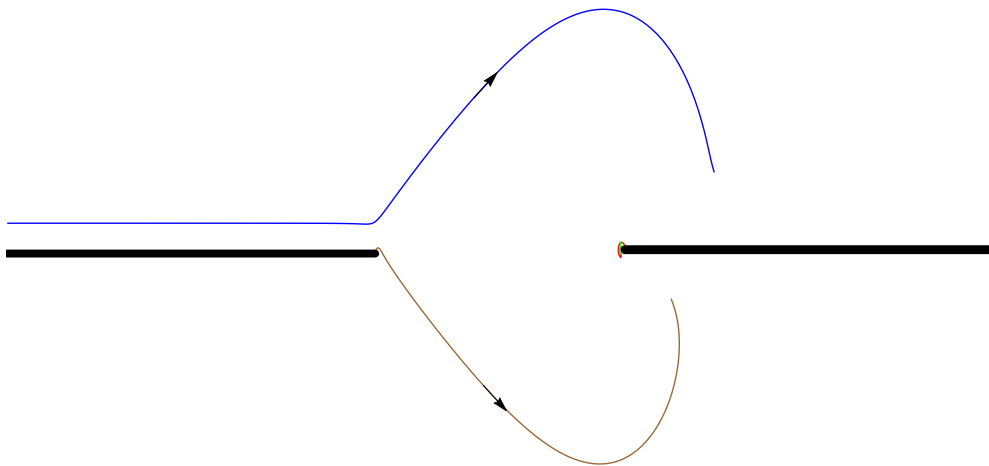

Figure 4.7: Trajectory of a vortex which begins at $z = -4 + 0.1i$, along with the trajectories of subsequent Brown-Michael vortices.

Chapter 5

Wedge Dynamics

We will now direct our attention to finding an analytical solution to the problem of steady flow past a wedge of arbitrary angle.

5.1 Conformal Map and Equations of Motion

The conformal map from the mathematical ζ-plane to the physical z-plane consisting of a wedge with exterior angle α is

$$\zeta = z^{\frac{\pi}{\alpha}}, \tag{5.1}$$

where we choose $\alpha \in (\pi, 2\pi)$ since we are not interested in the case of flow on the interior of a wedge where there is no sharp corner. When $\alpha \leq \pi$, the Kutta condition for a flow past the plate with complex velocity potential,

$$F(\zeta) = U\zeta, \tag{5.2}$$

can be satisfied since,

$$u - iv = \frac{dF}{dz} = \frac{\pi}{\alpha} U z^{\frac{\pi - \alpha}{\alpha}}, \tag{5.3}$$

which is finite at $z = 0$ since $\pi - \alpha \geq 0$, and therefore there is no singularity in the velocity field at the tip. If, however, $\alpha > \pi$ then the velocity does becomes singular at the tip of the wedge and therefore we require the Brown-Michael model to simulate the vortex shedding and we impose the Kutta condition.

It should be noted that in the limit $\alpha \to 2\pi$, we get the Cortelezzi problem (1995) reflected about the imaginary axis. In the limit $\alpha \to \pi$ we effectively have the identity map with no vortex shedding.

The complex velocity potential for the flow in the mathematical plane is no different from that in the Cortelezzi problem (3.1) since it is only the conformal map we have changed. Since $z^{\frac{\pi - \alpha}{\alpha}}$ becomes singular as $z \to 0$, the Kutta condition transforms to,
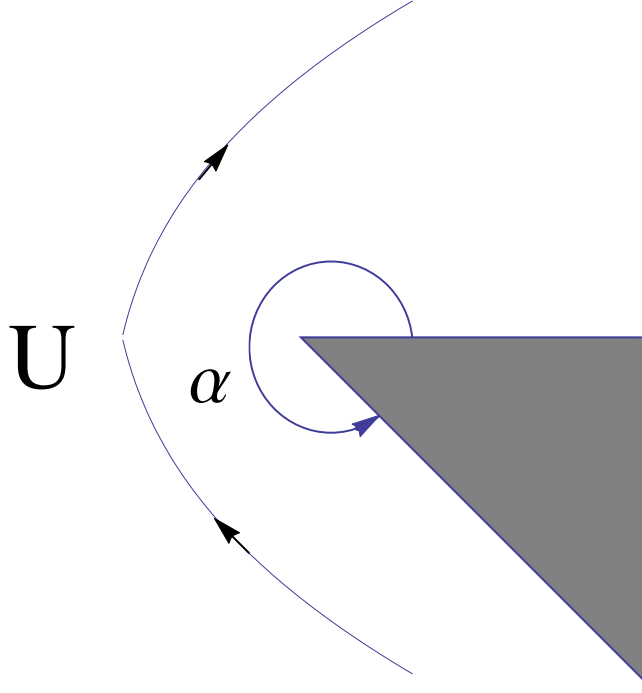
$$\frac{dF}{d\zeta} = 0, \quad \zeta = 0, \tag{5.4}$$

Figure 5.1: Steady flow U past a wedge of exterior angle α.

and therefore we derive an equation for the circulation $\Gamma_1(t)$ of the point vortex at position $\zeta_1(t)$ identical to (3.4). Thus, in the mathematical plane, the Brown-Michael equation (1.29) with initial position $z_{1_0} = 0$ becomes,

$$\frac{d\bar{\zeta}_1}{dt} - \frac{\pi}{\alpha}\bar{\zeta}_1\frac{|\zeta_1|^2}{\Im\zeta_1}\Im\left[\frac{1}{\zeta_1^2}\frac{d\zeta_1}{dt}\right] = U\frac{\pi^2}{\alpha^2}|\zeta_1^{1-\frac{\alpha}{\pi}}|^2\left(1 + \frac{|\zeta_1|^2}{4\Im\zeta_1}\left(i\frac{1-\frac{\alpha}{\pi}}{\zeta_1} - \frac{1}{\Im\zeta_1}\right)\right). \quad (5.5)$$

If we change to polar coordinates $\zeta = r_1 e^{i\theta_1}$ then (5.5) becomes,

$$\dot{r}_1 - ir_1\dot{\theta}_1 - \frac{\pi}{\alpha\sin\theta_1}\left(r_1\dot{\theta}_1\cos\theta_1 - \dot{r}_1\sin\theta_1\right)$$
$$= \frac{U\pi^2}{\alpha^2}r_1^{2\left(1-\frac{\alpha}{\pi}\right)}\left(e^{i\theta_1} + \frac{1}{4\sin\theta_1}\left(i\left(1-\frac{\alpha}{\pi}\right) - \frac{e^{i\theta_1}}{\sin\theta_1}\right)\right). \quad (5.6)$$

We then find the real and imaginary parts to be

$$\Re: \quad \dot{r}_1\left(1+\frac{\pi}{\alpha}\right) - r_1\dot{\theta}_1\frac{\pi}{\alpha}\cot\theta_1 = U\frac{\pi^2}{\alpha^2}r_1^{2\left(1-\frac{\alpha}{\pi}\right)}\cos\theta_1\left(1 - \frac{1}{4\sin^2\theta_1}\right), \quad (5.7)$$

$$\Im: \quad -r_1\dot{\theta}_1 = U\frac{\pi^2}{\alpha^2}r_1^{2\left(1-\frac{\alpha}{\pi}\right)}\sin\theta_1\left(1 - \frac{\alpha}{4\pi\sin^2\theta_1}\right), \quad (5.8)$$

which yield two coupled ordinary differential equations for r_1 and θ_1:

$$\dot{r}_1 = \frac{U\pi^2 (\alpha - \pi)}{\alpha^2 (\alpha + \pi)} r_1^{2\left(1 - \frac{\alpha}{\pi}\right)} \cos\theta_1, \tag{5.9}$$

$$\dot{\theta}_1 = \frac{U\pi^2}{\alpha^2 \sin\theta_1} r_1^{\left(1 - \frac{2\alpha}{\pi}\right)} \left(\cos^2\theta_1 + \frac{\alpha}{4\pi} - 1\right), \tag{5.10}$$

with initial conditions,

$$r_1(0) = 0, \quad \theta_1(0) = \theta_0 \in (0, \pi). \tag{5.11}$$

It should be noted that when $\alpha = 2\pi$, $(5.9 - 5.10)$ become (3.8) with constant U. The equations $(5.9 - 5.10)$ are singular at the initial position but we can use the dynamic rescaling suggested by McLaughlin et al (1986) to remove the singularity. We therefore make the following change of variables,

$$\xi = Ur_1^{\frac{2\alpha}{\pi} - 1}, \quad \omega = \cos\theta_1. \tag{5.12}$$

It follows from $(5.9 - 5.11)$ that,

$$\frac{d\xi}{dt} = \left(\frac{2\alpha}{\pi} - 1\right)\left(\frac{\pi^2 (\alpha - \pi)}{\alpha^2 (\alpha + \pi)}\right) U^2 \omega, \tag{5.13}$$

$$\frac{d\omega}{dt} = \frac{U^2\pi^2}{\alpha^2\xi}\left(1 - \omega^2 - \frac{\alpha}{4\pi}\right), \tag{5.14}$$

$$\xi(0) = 0, \quad \omega(0) = \omega_0 \in (-1, 1). \tag{5.15}$$

These combine to give,

$$\frac{\xi}{B}\frac{d^2\xi}{dt^2} + \left(\frac{d\xi}{dt}\right)^2 = \frac{C}{B}, \tag{5.16}$$

where we define the constants

$$B = \frac{\pi (\alpha + \pi)}{(\alpha - \pi)(2\alpha - \pi)}, \quad C = \left(1 - \frac{\alpha}{4\pi}\right)\frac{U^4\pi^3 (\alpha - \pi)(2\alpha - \pi)}{\alpha^4 (\alpha + \pi)}. \tag{5.17}$$

If we let $\phi = \frac{\xi}{B}$ then (5.16) becomes,

$$B^2 \left(\phi\frac{d^2\phi}{dt^2} + \left(\frac{d\phi}{dt}\right)^2\right) = \frac{C}{B}, \tag{5.18}$$

or,

$$\frac{d^2}{dt^2}\left(\phi^2\right) = \frac{C}{B^3}, \tag{5.19}$$

which we solve with the initial conditions to get,

$$\phi = \pm\sqrt{\frac{C}{B^3}}t, \quad \omega = \pm\frac{\alpha^2}{U^2\pi^2}\sqrt{CB} \quad (const), \tag{5.20}$$

or,

$$\xi = \pm\sqrt{\frac{C}{B}}t, \quad \omega = \pm\frac{\alpha^2}{U^2\pi^2}\sqrt{CB}, \tag{5.21}$$

where the sign of $\xi = Ur_1^{\frac{2\alpha}{\pi}-1}$ is determined by the sign of U and the sign of ω corresponds to the sign of ξ. Converting back to our coordinates (r_1, θ_1), we find,

$$r_1 = \left(\frac{|U|\pi(2\alpha-\pi)(\alpha-\pi)}{\alpha^2(\alpha+\pi)}\sqrt{1-\frac{\alpha}{4\pi}}t\right)^{\frac{\pi}{2\alpha-\pi}}, \tag{5.22}$$

$$\theta_1 = \cos^{-1}\pm\sqrt{1-\frac{\alpha}{4\pi}} \in (0,\pi). \tag{5.23}$$

Since $\alpha \in (\pi, 2\pi)$, we get,

$$\theta_1 \in \begin{cases} \in \left(\frac{\pi}{6}, \frac{\pi}{4}\right): & U > 0 \\ \in \left(\frac{3\pi}{4}, \frac{5\pi}{6}\right): & U < 0 \end{cases} \tag{5.24}$$

Finally, we use the transformation $z_1 = \left(r_1 e^{i\theta_1}\right)^{\frac{\alpha}{\pi}}$ to find the position of the vortex in the physical plane,

$$z_1 = \left(\frac{|U|\pi(2\alpha-\pi)(\alpha-\pi)}{\alpha^2(\alpha+\pi)}\sqrt{1-\frac{\alpha}{4\pi}}t\right)^{\frac{\alpha}{2\alpha-\pi}}e^{i\frac{\alpha}{\pi}\cos^{-1}\pm\sqrt{1-\frac{\alpha}{4\pi}}}. \tag{5.25}$$

Therefore, the vortex will move on a trajectory with a fixed angle $\lambda = \frac{\alpha}{\pi}\cos^{-1}\pm\sqrt{1-\frac{\alpha}{4\pi}}$, where,

$$\lambda \in \begin{cases} \in \left(\frac{\pi}{6}, \frac{\pi}{2}\right): & U > 0 \\ \in \left(\frac{3\pi}{2}, \frac{5\pi}{6}\right): & U < 0 \end{cases} \tag{5.26}$$

It is noted that $\Gamma_1 \propto t^{\frac{\pi}{2\alpha-\pi}}$ and therefore the circulation never reaches a stationary point. As long as the uniform stream is steady, there will only ever be one shed vortex. Vener (2004) investigated the same problem with a slightly different conformal map and an unsteady flow $U(t)$, though we both reached the same result in different ways. He derived the conditions by which there would be a circulation event for the first shed vortex forcing a second vortex to deploy from the tip.

5.2 Stability

If we let $\theta = \theta_0 + \xi(t)$, then (5.10) becomes

$$\dot{\xi} \approx -\xi\frac{2|U|\pi^2}{\alpha^2}\sqrt{1-\frac{\alpha}{4\pi}}r^{1-\frac{2\alpha}{\pi}}. \tag{5.27}$$

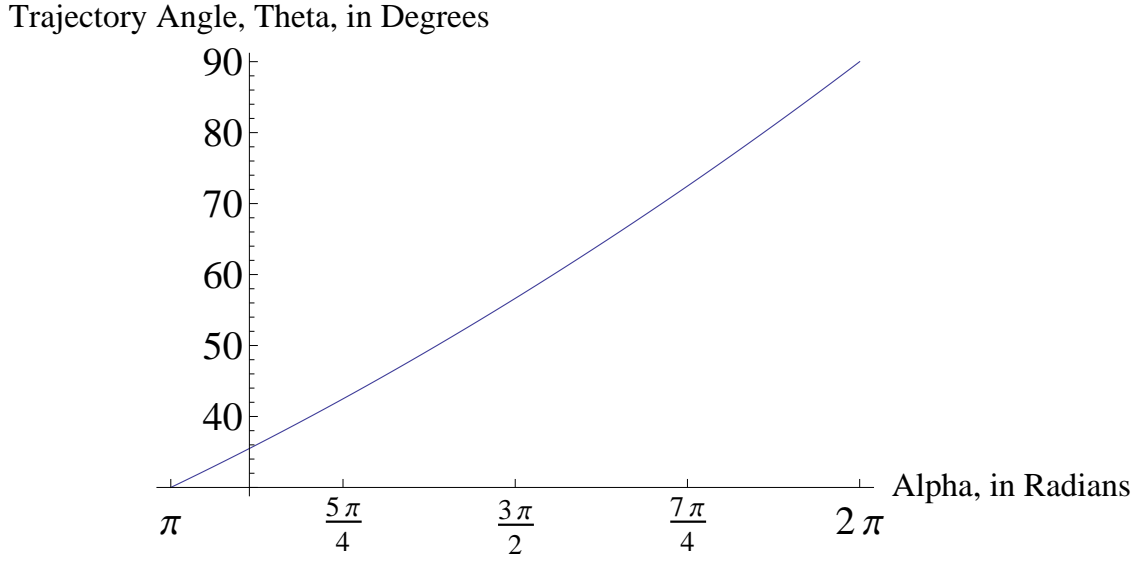We get an exponentially decaying perturbation and therefore the trajectory is stable.

Figure 5.2: Relationship between the wedge angle, α, and the trajectory angle, θ, of the shed vortex.

5.3 Wedge Angle-Trajectory Relationship

Having found an expression for λ, the angle of the trajectory of the shed vortex, it is of interest to investigate how this angle varies with respect to the wedge angle α. Without loss of generality, let's assume that $U > 0$, then the relation can be observed in figure (5.2).

5.4 Right Angle

In the case of $\alpha = \frac{3\pi}{2}$ the wedge becomes a right angle corner. In this scenario the position and circulation of the shed vortex are found to be,

$$z_1 = \frac{2 \cdot 2^{\frac{1}{8}} e^{i\frac{3}{2}\sec^{-1}\left(2\sqrt{\frac{2}{5}}\right)} (tU)^{\frac{3}{4}}}{3\sqrt{3} 5^{\frac{3}{8}}}, \tag{5.28}$$

$$\Gamma_1 = \frac{4\left(\frac{2}{5}\right)^{\frac{1}{4}} U\pi\sqrt{tU}}{3\sqrt{3}}. \tag{5.29}$$

The trajectory is plotted in (5.3). The vortex will move further and further away from the tip of the wedge at a fixed angle of $\frac{3}{2}\sec^{-1}\left(2\sqrt{\frac{2}{5}}\right)$ with increasing circulation since $\Gamma_1 \propto t^{\frac{1}{2}}$.
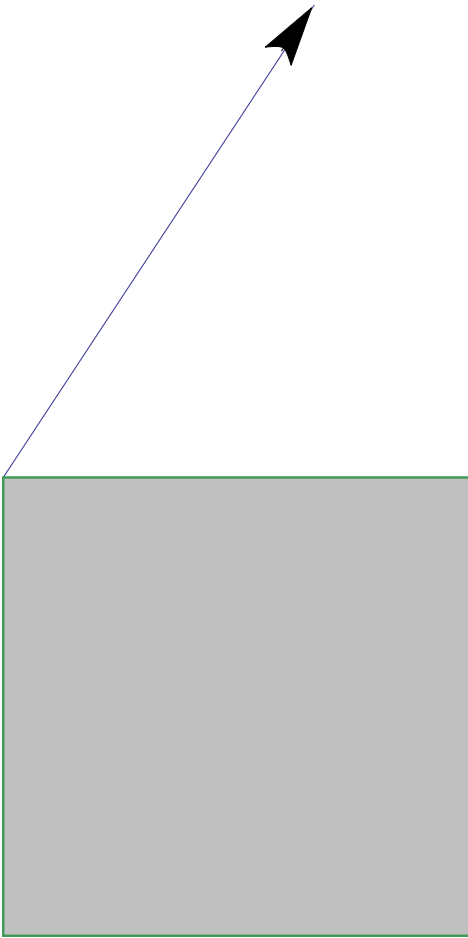
Figure 5.3: Vortex trajectory for the Brown-Michael model (1954) of flow past a right angled wedge, where $U = 1$. If we were to choose $U = -1$ then the trajectory would be in the opposite direction, i.e. reflected about the diagonal of the wedge.

Chapter 6

Conclusion

A variety of methods have been used to explore vortex dynamics in sharp edged domains. A vortex Hamiltonian approach was used to observe the path of a vortex near a gap in an infinitely long wall and near a semi-infinite plate. We found that a vortex which begins less than half the gap distance above the wall will slip through the gap and continue its path in reverse direction on the opposite side of the barrier. Otherwise it will jump across the gap and continue in the same direction. The superimposition of a background uniform stream was investigated and specific analysis was taken to observe the vortex dynamics very close to the sharp edge.

We then adopted the Brown-Michael model (1954) to simulate vortex shedding in several domains of interest. The first domain was a semi-infinite plate along the negative real axis. We followed Cortelezzi's method (1995) to find an exact solution for the position and circulation of a point vortex resulting from an unsteady flow past the plate. We found that the vortex will always move perpendicular to the plate on a stable trajectory either upwards or downwards depending on the sign of the uniform flow.

We then investigated the case of an oscillating flow past the plate, where the circulation of the shed vortex reached a critical maximum value after which it was forced to remain constant. A new vortex was then shed from the tip and the cycle repeated itself. Vortex after vortex was generated from the tip and many of them paired up as dipoles momentarily or permanently.

We then replaced the uniform flow with a flow driven by a vortex which initiates far down the length of the plate. We found that without the Brown-Michael model, the vortex would be driven along the wall by its image and then pass around the plate and continue on the opposite side in the reverse direction. However, when we acknowledge a second vortex shed from the tip of the plate, the path is completely different. The former vortex coming in from approximated $-\infty$ pairs up with the shed vortex of opposite sign and similar strength and together they form a dipole propagating away from the plate to infinity.

Reverting back to the original domain consisting of a gap in an infinitely long wall, we then adopted the Brown-Michael model to simulate vorticity shedding from the tips of the barriers. We investigated the case of a uniform stream through the gap and the consequent vortex shedding. We calculated the trajectories of the two vortices and found that they move almost perfectly perpendicular to the plate. By symmetry the two vortices have opposite sign and equal strength explaining why they propagate to infinity as a dipole.

We then replaced the uniform flow through the gap with a flow driven by a vortex initiating far down one side of the gap above the barrier. The flow generates a further vortex at each tip of the gap barriers. The result was that when the vortex coming in from approximated $-\infty$ approached the tip of the left hand wall it was repelled by the shed vortices such that it jumped across the gap. We attempted placing the starting vortex $\frac{1}{20}$ of the gap distance above the wall and it still persisted in jumping over. Contrasting the results from the Hamiltonian methods, it would appear that the vortex jumps across no matter how close we might initiate it above the wall.

We finally applied the Brown-Michael model to the steady flow past a wedge of arbitrary angle, where a point vortex is shed from the tip of the wedge. We derived an exact solution for the position of the vortex in terms of the wedge angle. It was found that the vortex will always move on a trajectory with fixed angle θ and we were able to plot a relationship between the wedge angle and the trajectory angle. In the specific case of a right angle wedge we derived the vortex position and circulation.

The Brown-Michael model could be considered idealised and unrealistic, yet Brown and Michael (1954) compared their simulated results for the velocity and pressure of the fluid near a delta wing to experimental results and found a strong correlation.

There are numerous further domains and fluid flow examples which could be explored. Llewellyn-Smith (Llewellyn-Smith, 2009) has used this model to simulate the effect of vortex shedding on a falling card. In that problem the location of the boundary, as well as the shed vortices, must be found. Vener (2004) derived the vortex dynamics for an unsteady flow past a corner of arbitrary angle, and considering that any polygon is made up of sharp corners, one could potentially approximate the effect of vortex shedding on a falling 2-dimensional shape. As the object fell, unsteady flow past the shape corners would generate a series of vortices which in turn would alter the position and rotation of the object.

Acknowledgments

I would like to thank Robb McDonald for supervising my project and for the numerous interesting conversations and the encouraging advice. I would also like to thank University College London for providing a nourishing environment to work and an overall fantastic degree experience.

Chapter 7

Bibliography

G. R. Baker. A test of the method of fink soh for following vortex-sheet motion. *J . Fluid Mech. (1980)*, 100, part 1:209–220, 1980.

C. E. Brown. Effect of leading-edge separation on the lift of a delta wing. *Journal of the Aeronautical Sciences (Institute of the Aeronautical Sciences) 21, No. 10 (1954)*, 21:690–694, 1954.

L. Cortelezzi. On the unsteady separated flow past a semiinfinite plate: Exact solution of the brown and michael model, scaling, and universality. *Physics of Fluids 7, 526 (1995)*, 7:526, 1995.

S. Michelin ; S. Llewellyn-Smith. An unsteady point vortex method for coupled fluid-solid problems. *Theoretical and compuatation Fluid Dynamics (2009)*, 23:150–152, 2009.

E. R. Johnson ; N. Robb McDonald. The motion of a vortex near a gap in a wall. *Physics of Fluids 16, 462 (2004)*, 16:462, 2004.

D. W. McLaughlin, G. C. Papanicolaou, C. Sulem, and P. L. Sulem. Focusing singularity of the cubic schrdinger equation. *Phys. Rev. A*, 34:1200–1210, Aug 1986.

P. G. Saffman. *Vortex dynamics*. Cambridge : Cambridge University Press, 1995.

D. Vener. Two-dimensional vortex shedding from a corner. *Woods Hole Oceanographic Institute*, 2004.